

## **Response of Microplankton Size Structure to Summer Stratification, Freshwater Influx and Coastal Upwelling in the Southeastern Arabian Sea**

**Karnan, C., \*Jyothibabu, R., Arunpandi, N., Albin Jose., Parthasarathi, S., Santhi Krishnan, S**

CSIR-National Institute of Oceanography, Regional Centre, Kochi, India

Corresponding author. Telephone: +91 484 2390814; Fax: +91 484 2390618

\*E-mail address: rjyothibabu@nio.org

### **Abstract**

A year-round FlowCAM-based study of micro-plankton (20-200 $\mu\text{m}$ ) size structure was conducted in several locations along a cross-shore transect off Kochi in the near-shore waters of the southeastern Arabian Sea (SEAS; along the southwest coast of India). The study area was characterized by a warmer and thermally stratified water column during the Pre-Southwest Monsoon (PSWM; March to May), which was replaced by the cool and hypoxic upwelled waters at the sub-surface and low salinity estuarine waters at the surface during the Southwest Monsoon (SWM; June to September). Irrespective of seasons, micro-autotrophs displayed higher abundance and biomass closer to the coast as compared to the offshore locations. The seasonal trend in the abundance and biomass of micro-autotrophs mismatched in the study region, the former was the highest (av. 8430  $\pm$  2927 ind/L and av. 10.3  $\pm$  2  $\mu\text{gC/L}$ ) during the PSWM and the latter during the SWM (av. 7703  $\pm$  1237 and av. 16.8  $\pm$  3.5  $\mu\text{gC/L}$ ). Micro-autotroph biomass was found to be higher in the surface waters, with an exception during the SWM, when larger micro-autotrophs (av. 137184  $\pm$  10196  $\mu\text{m}^3/\text{ind.}$ ) were observed in the subsurface. The highest seasonal abundance of micro-autotrophs (av. 8430  $\pm$  2927 ind/L) during the PSWM could be attributed to the presence of smaller individuals (biovolume av. 59801  $\pm$  6906  $\mu\text{m}^3/\text{ind.}$ ). The overall spatial distribution of micro-heterotrophs was similar to that of the micro-autotrophs, with their high abundance and biomass in locations closer to the coast. Also, their abundance was found to be higher throughout the water column during PSWM, while it decreased noticeably in the deeper waters during the rest of the period. During the SWM, low PAR, high nutrients and high salinity in the sub-surface waters facilitated the dominance of larger micro-autotrophs (diatoms) such as *Fragilaria* (av. 211093  $\pm$  8431  $\mu\text{m}^3/\text{ind.}$ ) and *Thalassiosira* (av. 80027  $\pm$  5031  $\mu\text{m}^3/\text{ind.}$ ), whereas low salinity and high nutrient water mass from the adjacent Cochin (Kochi) backwaters favored high abundance of smaller micro-autotrophs such as *Thalassionema* (av. 17220  $\pm$  756  $\mu\text{m}^3/\text{ind.}$ ) and *Skeletonema* (av. 11831  $\pm$  533  $\mu\text{m}^3/\text{ind.}$ ) in the surface water. This study evidences for the first time that due to temporal changes in water masses in the near-shore waters in the SEAS, there are considerable seasonal and spatial variations in the size structure and composition even within the micro-plankton community itself.

**Keywords:** Micro-plankton, Size structure, Upwelling, Southeastern Arabian Sea, FlowCAM

## 1. Introduction

The temporal and spatial changes in hydrography can significantly alter the abundance, composition and size structure of plankton in marine systems (Banse, 1982; Pomeroy, 2007), which in turn can impart significant ecological implications on the lower level food web (Sieburth et al., 1978; Azam et al., 1983). The nutrient enriched coastal waters promote the growth of large (>20µm; micro and meso size) phytoplankton, whereas, nutrient depleted environments promote smaller (<20µm; pico and nano) phytoplankton (Subrahmanyam, 1959; Banse, 1982; Landry et al., 1998; Karnan et al., 2017a). The large phytoplankton (20-200µm) are consumed by large organisms such as zooplankton and fish, resulting in a short food chain with high trophic efficiency making coastal waters highly productive (Marshall, 1973; Sieburth et al., 1978; Johnson and Sieburth, 1982; Azam et al., 1983; Ward et al., 2012; Jyothibabu et al., 2018). Therefore knowing how environmental variability influences the size structure of phytoplankton in coastal waters is important for the correct management of resources in these areas.

Fishing is an important socioeconomic activity in the nearshore waters along the southwest coast of India. During the Pre-Southwest Monsoon (PSWM; March to May), the SEAS is significantly warmer with very weak winds, consequently having a thermally-stratified water column. During this period, the abundance and biomass of the micro-autotrophs in the SEAS as a whole is relatively low compared to the rest of the period due to the low availability of essential nutrients (Gauns et al., 2005; Jyothibabu et al., 2008). During the Southwest Monsoon/ Summer Monsoon (SWM; Jun.-Sep.), the oceanic southwesterly winds in the open Arabian Sea blow as westerly/northwesterly (>7 m/s) along the south Indian coastline and favor an offshore (Ekman) transport causing upwelling of subsurface waters (50-90 m) along the coast (Hareeshkumar and Anand, 2016 and references therein). Studies have also showed there are some remote forcing through Kelvin waves as the causative factor of the coastal upwelling and its northward propagation along the southwest coast of India (Shankar and Shetye, 1997; Smitha et al., 2008). The coastal upwelling increases the nutrient concentrations leading to a noticeable increase in autotrophic plankton production in the surface layers (Bhattathiri et al., 1996; Qasim 1982; Madhupratap et al., 1990; Jyothibabu et al., 2008; Karnan et al., 2017a). On the other hand, the Northeast Monsoon (NEM; November - February) is characterized by a moderate north-easterly wind, which is not strong enough to break the salinity stratification in the south-eastern Arabian Sea caused by the intrusion of Bay of Bengal waters (Wyrski, 1973; Sanilkumar et al., 2004). Hence, nutrient availability in the ocean surface layer is scarce, leading to a significantly low phytoplankton production (Madhupratap et al., 1996; Jyothibabu et al., 2010).

The large scale seasonal hydrographical settings in the SEAS mentioned above might not be exactly applicable to the nearshore waters due to its proximity to the coastline. This is particularly significant during the SWM, when there is a large freshwater influx into the sampling area (Simon and Mohan Kumar, 2004; Jyothibabu et al., 2008; Anjusha et al., 2018a). This freshwater plume from the adjacent estuary (Kochi backwaters) creates a surface low saline lid over the upwelled waters (Banse, 1968; Ramamirtham and Jayaraman, 1960). Thus, the overall enhancement of plankton biomass in the near shore waters along the southwest coast of India during the SWM is the sum of nutrient enrichment caused by coastal upwelling and estuarine influx (Madhupratap et al., 1990; Nair et al., 1992). By other hand, the NEM is characterized by moderate rainfall and low nutrient influx from the land/estuary into the near-shore waters. However, as the season advances to the PSWM period, the nutrient supply from the estuary decreases, and thus the entire coastal region remains nutrient-depleted leading to significantly low phytoplankton stock (Bhattathiri et al., 1996; Qasim, 2003; Jyothibabu et al., 2008). The tidal activity may also cause some impact on plankton production in the nearshore waters, though its effect is still unknown.

Studies on the seasonality of micro-plankton size structure along the southwest coast of India are very limited (Karnan et al., 2017a, b). Here we show a monthly sampling carried out in the near shore waters of Kochi, where coastal upwelling and large estuarine influx occurs simultaneously during the SWM (Jyothibabu et al., 2008). Along with classical oceanographic observations, this study utilized a FlowCAM (Sieracki et al., 1998; Alvarez et al., 2013; Karnan et al., 2017c) to understand how seasonal hydrographical features such as summer stratification, freshwater influx and coastal upwelling influence the microplankton size structure and composition in the near-shore waters along the southwest coast of India. The main objectives of this study in the near shore waters along the south west coast of India are (a) to quantify the size structure of autotrophic microplankton as a response to seasonal hydrographical transformation, (b) to infer how seasonal hydrographic variability and plankton size structure influence the food web and higher trophic levels.

## **2. Materials and methods**

### **2.1. Sampling methods**

A monthly time series sampling was carried out along a cross-shore transect off Kochi. 8 locations were selected along a cross-shore transect between 6m and 30m depth contours. Field sampling was carried out using a fishing trawler *Santa Cruz* for one year from January - December 2014 (Figure 1). In all locations (1 to 8), a Conductivity Temperature Depth (CTD, SBE 911 Plus, Seabird Electronics, USA) profiler equipped with a few additional sensors was used to record the high

resolution vertical distribution (from every 0.2m water depths; CTD lowering speed was ~0.1m/s) of temperature, salinity, turbidity, PAR and chlorophyll *a*. Water samples for chemical and plankton parameters were collected from 4 locations (1, 3, 5 and 7) using Niskin samplers. At each location, three depths (surface, middle and bottom) were sampled except in shallower (6m) location. The mid depth was determined based on total depth of the corresponding station. It was 6m at location 3, 10m at location 5, and 13m at location 7. The dissolved oxygen was measured following Winkler's titration method and major nutrients (nitrate, phosphate and silicate) were analyzed following standard protocols (Grasshoff et al., 1983). For microplankton size structure and composition, 0.2 - 1L of water from different depths were analyzed using a FlowCAM following standard practices (Karnan et al., 2017a). Sampling exercise failed in June due to very rough sea condition. Similarly, November sampling is not represented in this paper due to an error in CTD data.

## **2.2. FlowCAM analysis**

Based on the particle concentration in the water, varying volumes of samples (200ml - 1L) were processed for FlowCAM analysis. Water samples collected were pre-filtered using a 300 $\mu$ m bolting silk and then concentrated with a 20 $\mu$ m bolting silk filter fixed on a rubber tubing, to 20ml, details of this is described in Karnan et al., (2017a). A portable FlowCAM - VS4 (Sl. No. 614) was used to analyze the concentrated samples. A 300 $\mu$ m flow cell with 100% field of view with the combination of 4X objective was used in this analysis. The images of unwanted particles were removed and good quality plankton images (>20 $\mu$ m ESD) were classified to the genus level with the help of inbuilt algorithms. This is useful in sorting particles based on their morphological measurement values and automatic selection of particles based on the statistical similarity of selected particles ( $\geq 2$ ). The transparent frustules of diatom cells were considered as dead cells and they were removed from the count. The Estimated Spherical Diameter (ESD) volume was not preferred in the present analysis because most of the autotrophs showed long filaments, hooks and setae, and in such cases, ESD volume calculations lead to overestimations (Karnan et al., 2017c). The plankton biomass of each individual was estimated based on Area Based Diameter (ABD) volume algorithm and numerical conversion factors available in standard literatures (Verity and Langdon, 1984; Verity et al., 1992; Michaels et al., 1995; Menden-Deuer and Lessard, 2000; Tada et al., 2000; Gowing et al., 2003; Marquis et al., 2011). The particle shape was estimated from the aspect ratio (AR) of each plankton (Olson, 2011a,b; Alvarez et al., 2012; Caromel et al., 2014; Karp-Boss and Boss, 2016). The AR was calculated from the length (Feret's maximum length; F mxl) and width (Feret's minimum length; F mnl) measurement of each individual plankton ( $AR = F\ mnl / F\ mxl$ ). The AR algorithm is available in the visual spreadsheet of FlowCAM.

### 2.3. Data analysis

Normal Q-Q probability plots and Shapiro-Wilk normality test were used for selected hydrographical parameters (temperature and salinity) to understand their theoretical distribution pattern (Becker et al., 1988; Royston, 1995; R Core Team, 2018). Bartlett's test was performed to estimate the variance in each individual parameter. To understand the spatial and temporal variances in major hydrographical parameters, Tukey's HSD and Dunn's test (Bonferroni method) were carried out (Chambers and Hastie., 1992; Yandell, 1997; R Core Team, 2018). Multivariate analysis (hierarchical clustering and nMDS) was used for grouping/clustering of samples based on locations and seasons, depending on the similarity in their physico-chemical parameters. The interrelationships between various physico-chemical and biological parameters were analyzed based on redundancy analysis (RDA) available in CANOCO 4.5 software. The result of RDA analysis has been presented as triplots in which samples are represented as points, and quantitative environmental and biological variables as arrows. The direction of an arrow in a triplot indicates the direction of increase of that variable and the angle between two arrows represents how significantly they are correlated (Leps and Smilauer, 2003). The RDA Triplots were developed along with *r* matrix to depict the correlation among environmental and biological parameters (Friendly, 2002; R Core Team, 2018).

## 3. RESULTS

### 3.1. Hydrography

#### 3.1.1. Temperature

The temperature in the sampling domain was significantly different during the three seasons ( $p < 0.001$ ), with the surface temperature showing  $\sim 4^\circ\text{C}$  of variation seasonally (Figure 2a). The water column remained warm from February to May with the highest temperature in April ( $>30^\circ\text{C}$ ). In May, there was clear indication of cool bottom waters along the sampling transect. Due to technical reasons, CTD data for June was not available and, therefore, the signatures of cool water ( $26^\circ\text{C}$ ) in the subsurface were continuously available only from July onwards. The surface temperature (1m) of adjacent locations were not significantly different, but alternative locations were emphatically so (ANOVA  $p\text{-value} < 0.005$ ,  $df=35$ ). The temperatures of near-bottom waters during July and September dropped as low as  $23^\circ\text{C}$ . The difference in temperature in the surface and bottom waters was significant during the PSWM and SWM periods ( $p < 0.005$ ).

#### 3.1.2. Salinity

During the PSWM, the entire sampling region showed high salinity water ( $>34$  PSU) (Table 1). The near-bottom waters of offshore locations showed a high salinity tongue ( $>35$  PSU) extending

towards the coast in May. July in the SWM period received the highest rainfall (678 mm), which created a low salinity plume in the sea surface (Figure 2b). In July, there was a 5-10m thick layer of low salinity water mass (<33 PSU) in the surface waters along the transect. The thickness of this low salinity water in the surface along the sampling transect was the highest closer to the coast. A high salinity water mass extending towards the coast through the subsurface was the general feature throughout the SWM; however, from October onwards, this high salinity water mass retreated from the subsurface and disappeared completely by the onset of the NEM. The sea surface salinity during the SWM significantly varied (ANOVA p-value<0.001, df = 8) from those during the PSWM and NEM seasons, though the water column salinity variations between PSWM and NEM were insignificant (ANOVA p-value >0.2). The salinity variation between surface and bottom waters was found insignificant (p>0.05) during the NEM, but it was significant during the PSWM and the SWM (p<0.002). Stratification in the water column was stronger during the SWM and relatively weaker during the PSWM (Figure 2c). Irrespective of the sampling period, locations closer to the coast were more regularly influenced by the low salinity estuarine water mass, and showed vertical stratification.

#### **3.1.4. Photosynthetically Available Radiation (PAR) and Turbidity**

The euphotic column was relatively deeper from January to May due to the availability of high solar radiation. The highest PAR (>1000  $\mu\text{E}/\text{m}^2/\text{S}$ ) was observed during the PSWM period. During the SWM, solar radiation decreased, causing the shallowest euphotic depth (Supplementary Figure 1). Especially in July and September, the euphotic depth was significantly shallow as the light attenuated within a very thin surface layer. From October, light penetration in the water column gradually increased and high PAR was available in the subsurface waters. Turbidity has an important role in underwater PAR, which was much lower during NEM and PSWM in the study region compared to the SWM ( $4.59 \pm 1.26$  NTU).

#### **3.2. Nutrients and Dissolved Oxygen**

Nitrate ( $\text{NO}_3$ ) concentration was the lowest during the PSWM and moderate during the NEM (Figure 3). Seasonal mean of horizontal and vertical distribution of  $\text{NO}_3$  showed a decreasing trend in concentration from the coastal to the offshore location; the highest mean concentration was observed during the SWM season (av.  $6.56 \pm 1.71$   $\mu\text{M}$ ). The concentration of  $\text{NO}_3$  during the NEM (av.  $0.89 \pm 0.15$   $\mu\text{M}$ ) and the PSWM (av.  $0.88 \pm 0.11$   $\mu\text{M}$ ) was quite comparable (Table 1). Nitrate concentration in the water column showed a general increasing trend from the surface to bottom during all seasons (Figure 3b). Phosphate concentration in the sampling region showed a slight

decrease in concentration from coastal to offshore locations, irrespective of the sampling period. Vertically, higher phosphate concentration was found near the bottom, followed by the surface and mid-depth waters (Figure 3; Supplementary Table 1). Silicate concentration was always high in the study domain, irrespective of seasons.

Dissolved oxygen concentration in the study domain was found to be higher during the NEM compared to the other seasons (Table 1 & Supplementary Table 1). During the PSWM, the dissolved oxygen concentration in the water column was moderate (av.  $4.33 \pm 0.44$  ml/L). During the SWM, surface waters showed high concentration of dissolved oxygen (av.  $7.1 \pm 1.2$  ml/L), whereas subsurface waters had significantly low oxygen values (av.  $3.4 \pm 1$  ml/L). Hypoxic waters were found in the deeper layers during the SWM as a result of coastal upwelling; in July, bottom waters received significantly low oxygenated mid-depth oceanic water masses (av.  $1.4 \pm 1.2$  ml/L) through coastal upwelling (Table 2).

### **3.3. Biological parameters**

#### **3.3.1 Chlorophyll *a***

Chlorophyll *a* concentration in the study area was always higher at locations closer to the coast (Figure 4). Vertical distribution of chlorophyll *a* in the water column showed high values in the surface layers. Chlorophyll concentration was generally low during the PSWM. However, high chlorophyll of limited stretch was evident in the surface during March and April. The patch during March was caused by its export from the estuary, while that during April was caused by *Trichodesmium* bloom. Later in July, chlorophyll *a* concentration increased significantly throughout the water column, though a relatively low chlorophyll condition was observed in August. In September, chlorophyll concentration reached its seasonal peak, with the top 10m water column showing significantly high chlorophyll *a* concentration ( $>4$  mg/m<sup>3</sup>). Subsequently, chlorophyll concentration in the water column decreased from October (Figure 4; Table 2).

#### **3.3.2 Autotrophic micro-plankton**

##### **3.3.2.1. Abundance and biomass**

Microautotrophs abundance generally showed noticeable seasonal variation (Figure 5; Table 1 & Supplementary Table 1). In location near the coastline (location 1; 6m), the abundance of microautotrophs was maximum during the PSWM (av.  $19607 \pm 10974$  ind./L), followed by the SWM and the NEM. The micro-autotrophs abundance was always high in the surface, while the abundance peaked in the surface and bottom during the SWM (Figure 5b). The surface waters showed maximum abundance (av.  $16197 \pm 7445$  ind./L) during the PSWM followed by the NEM and the

SWM. During the PSWM, *Skeletonema* sp. contributed more than 80% of the total micro-autotroph abundance, followed by *Leptocylindrus* sp. and *Chaetoceros* sp. *Thalassiosira* sp. and *Fragilaria* sp. were dominant during the SWM. The autotrophs were low during the NEM, when *Chaetoceros* sp., *Pseudo-nitzschia* sp. and *Skeletonema* sp. were the dominant species (Supplementary Table 2).

There was a noticeable variation in the distribution of micro-autotrophs (Figure 5). Similar to chlorophyll *a*, the mean abundance and biomass of micro-autotrophs decreased from the coastal to the offshore locations, irrespective of seasons. During the PSWM and the NEM, the spatial distribution of micro-autotrophs was almost similar, while it was different during the SWM (Figure 5a, 5b). The biomass decreased from inshore to offshore locations. The mean biomass was lowest during NEM, moderate during PSWM and highest during SWM, whereas the mean biomass was highest in the bottom (av.  $19.7 \pm 6.7 \mu\text{gC/L}$ ) during the SWM, followed by surface (av.  $12.2 \pm 2.58 \mu\text{gC/L}$ ). Overall, the mid depth showed low abundance and biomass of micro-autotrophs (Supplementary Table 1). Supplementary Figure 2a-c shows the FlowCAM images of dominant autotrophs during different seasons.

### 3.3.2.2. Size structure

The mean size of micro-autotrophs noticeably varied on temporal and spatial scales (Figure 6, Supplementary Table 1 & 3). In general, the mean body size of micro-autotrophs was smallest in the low salinity waters found inshore and at the surface, as compared with the offshore and subsurface waters. The horizontal size distribution of micro-autotrophs showed an increasing trend in their mean biovolume from inshore to the offshore locations, irrespective of seasons. In general, relatively large-sized micro-autotrophs were found in the study area during the SWM, and more in the offshore locations (av.  $97716 \pm 12603 \mu\text{m}^3/\text{ind.}$ ) as compared to the inshore ones (av.  $75769 \pm 20368 \mu\text{m}^3/\text{ind.}$ ). During the SWM, highest micro-autotroph size was recorded in September in the bottom waters (Table 2).

Vertical distribution of micro-autotrophs in all seasons showed an increasing trend in body size from surface to bottom (Figure 6b; Supplementary Table 1 & 3). Microplankton mean size was smaller at the surface during the NEM and PSWM as compared to the bottom waters. During the SWM season, micro-autotroph size was smaller in the surface waters (av.  $56468 \pm 9104 \mu\text{m}^3/\text{ind.}$ ), mid-depth waters were inhabited by relatively larger individuals (av.  $128305 \pm 48980 \mu\text{m}^3/\text{ind.}$ ) and the bottom waters showed the presence of the largest individuals (av.  $137184 \pm 10196 \mu\text{m}^3/\text{ind.}$ ).



### 3.3.2.3. Shape and size class

The major shapes of plankton such as spherical, elliptical and needle shape were derived from the AR of individual plankton (Figure 7a-c). During the NEM, 82% of the total autotrophs were needle shaped (AR <0.4), 10% were elliptical (AR 0.4-0.6) and 8% were spherical (AR >0.6). During the PSWM, the needle shaped autotrophs dominated (86%), followed by 9% of elliptical and 6% of spherical plankton. Later during the SWM, needle shaped plankton contribution decreased (56%) whereas, the abundance of elliptical (23%) and spherical (22%) plankton have increased. Very few species (*Thalassiosira* sp., *Coscinodiscus* sp.) were represented under spherical category and their number increased significantly during the nutrient rich SWM season.

The autotrophic plankton components were grouped under three size classes (Figure 7d-f), such as <40µm (smaller), 40-60µm (medium) and >60µm (larger). During all seasons, the more abundant smaller autotrophs (<40µm) contributed less to the total autotrophic biovolume compared to the less abundant larger autotrophs (>60µm). A sizable quantity of the micro-autotroph biomass was found to be larger in size (Figure 7d-f) especially during the SWM, when it was supported by nutrient enrichment (Figure 7).

### 3.3.3. Heterotrophic micro-plankton

#### 3.3.3.1. Abundance and Biomass

The abundance and biomass of micro-heterotrophs also showed noticeable temporal and spatial variations (Figure 8; Supplementary Table 1). Throughout the sampling period, the coastal waters contained higher abundance and biomass of micro-heterotrophs compared to the remaining locations (Figure 8a). During the PSWM, the abundance of micro-heterotrophs in the inshore region (location 1) was higher (av.  $2303 \pm 313$  ind./L) as compared to the offshore locations (av.  $278 \pm 58$  ind./L). Similarly, during the NEM, inshore locations showed higher abundance of micro-heterotrophs (av.  $1068 \pm 262$  ind./L) compared to the offshore (av.  $162 \pm 35$  ind./L). During the SWM, the low salinity coastal water (location 1) showed noticeably higher abundance of micro-heterotrophs (av.  $1317 \pm 596$  ind./L). The SWM seasonal micro-heterotroph community was mainly dominated by copepod nauplii and *Protoperidinium* (Supplementary Table 2; Figure 8). Their abundance was high in the surface and bottom as compared to the mid depth during the PSWM (Figure 8b). There was a notable decrease in the mid and bottom as compared to the surface during the SWM (Figure 8b). The lowest seasonal abundance of micro-heterotrophs was found during the NEM.

The microheterotrophs biomass followed the same trend as their abundance (Figure 8a), with maximum in the inshore region during the PSWM (av.  $25.4 \pm 3.5$  µgC/L); however, the biomass in

the offshore region was low during the same period (av.  $3.1 \pm 0.4 \mu\text{gC/L}$ ). The offshore waters showed relatively high micro-heterotrophs biomass only during the SWM. The biomass was maximum during the PSWM (surface av.  $9.43 \pm 3.62 \mu\text{gC/L}$  and bottom av.  $8.83 \pm 2.54 \mu\text{gC/L}$ ; Figure 8b). Supplementary Figure 2d-f shows the FlowCAM images of dominant micro-heterotrophs during different seasons.

### 3.3.3.2. Size structure

Throughout the sampling period, the size of the micro-heterotrophs increased from the inshore to the offshore waters (Figure 9, Supplementary Table 1 & 3). During the NEM, the micro-heterotrophs in the inshore waters showed relatively smaller biovolume (av.  $157897 \pm 27152 \mu\text{m}^3/\text{ind.}$ ) as compared to the offshore waters (av.  $215781 \pm 32316 \mu\text{m}^3/\text{ind.}$ ). Similar trend was observed during the NEM and the PSWM seasons (Supplementary Table 1). Spatially, a wider range of body size of micro-heterotrophs was found during the SWM ( $137857 \pm 41784 \mu\text{m}^3/\text{ind.}$  at the inshore location and  $279834 \pm 44552 \mu\text{m}^3/\text{ind.}$  at the offshore one). The body size distribution of micro-heterotrophs in the water column showed only a marginal difference in mean body size in the surface, mid and bottom waters, irrespective of seasons; marginally larger-sized micro-heterotrophs were found in the mid-waters during all seasons (Supplementary Table 1).

### 3.4. Statistical Analysis

The ecological effects of different hydrographical settings in the study domain and their effect on chlorophyll *a* and micro-plankton parameters (size and biomass) was evident in RDA Triplots (Figure 10). Triplots clearly showed the enrichment of nutrients and a significant increase in autotrophic components during the SWM. The reverse situation was evident in sampling locations during the PSWM and NEM, characterized by increased temperature, salinity and PAR (Figure 10). From onshore to offshore, the abundance and biomass of autotrophs showed negative correlation ( $p < 0.05$ ) with physical parameters and positive with nutrients ( $p < 0.05$ ), as illustrated in the correlogram (Figure 10b). In the vertical water column, size and biomass of autotrophs showed negative correlation with temperature and positive correlation with nutrients (Figure 10d).

## 4. Discussion

Studies have shown that the physical signatures of coastal upwelling in the eastern Arabian Sea are discernible in the deeper Indian shelf waters by the early PSWM (March) itself (Shenoi et al., 2005; Gupta et al., 2016). As the biological signatures of coastal upwelling become evident by June in the inshore waters, traditionally and from a biological stand point, the upwelling period is considered from June to September (Banse, 1959; Habeebrehman et al., 2008; Jyothibabu et al.,

2010; Karnan et al., 2017a). The present study area is located in the coastal waters of Kerala, which is the southwestern state of India bordered by the Arabian Sea in the west and the Western Ghats (mountain ranges) in the east. Meteorologists consider Kerala as the “Gateway of Summer Monsoon” (Krishnakumar et al., 2009; Narayanan et al., 2016). The moisture-laden winds from the Arabian Sea get partly hindered by Western Ghats (~2000m), leading to the heavy rainfall over Kerala (Simon and Mohankumar, 2004; Krishnakumar et al., 2009; Narayanan et al., 2016). The rainfall on the windward slopes of the Western Ghats is drained into the nearshore waters of the southwest coast of India by numerous rivers (Simon and Mohankumar, 2004). The Kochi backwater/estuarine system is the largest of its kind along the west coast of India, which receives freshwater from seven rivers (Jyothibabu et al., 2006). These influxes from the Kochi backwaters produce vertical stratification in the present study area (off Kochi) particularly during the SWM.

It was observed that the semi-annually reversing wind is the major factor regulating the heat exchange in the mixed layer through evaporative cooling, vertical mixing, warming and coastal upwelling in the present study area (Muraleedharan and Prasanna Kumar, 1996; Jyothibabu et al., 2010). It is clear in the present data that warm waters were present near the coastal locations as compared to the offshore locations, which was indicating the intrusion/advection of warm estuarine waters in the inshore region. It was observed earlier that upwelling in the near shore region was restricted to the subsurface by a cap of freshwater coming from the estuary (Banse, 1968; de Souza et al., 1996; Jyothibabu et al., 2008). The freshwater influx from the estuary against the strong upwelling could create a strong stratification in the near shore waters of the present study region during SWM. Thus, upwelling gets restricted only to the subsurface in the near shore regions during SWM, and the intensity of this inhibition decreases towards offshore. With the retreat of monsoon rains, the estuarine influx can still influence the surface salinity in the inshore region, though its effect on the stratification is very weak during that period (Figure 11a).

As mentioned above, the high river flux during the SWM causes density stratification (salt wedge) in the coastal waters of Kochi. This case was noticed first in the study area by Ramamirtham and Jayaraman (1960) who observed subsurface cool water overlaid by low saline warm water during the SWM due to the coastal upwelling in the subsurface and freshwater influx in the surface layers. They also noticed in the Cochin inlet region, a 10m low saline surface layer spreading towards offshore over the high salinity tongue below. Ramamirtham and Jayaraman (1963) further noticed the intrusion of the upwelled water mass into the Kochi backwaters through the shipping channel in the inlet. In the present study, this was not observed as the present location closest to the coastline (6m depth) was somewhat away from the shipping channel. The possible impact of low oxygenated water

in the subsurface and its influence on plankton and fishes are represented schematically in Figure 11b. During upwelling period, the stratification coupled by offshore advection of low saline surface waters may be the main mechanism to balance the hydrological pressure gradients in the environment (Ramamirtham and Jayaraman, 1960). This is pertinent in the context that the prevailing wind during the SWM is incapable in eroding the density stratification caused by huge freshwater influx during that period. Tidal force may also favor a piling up of low saline waters near the coastline, but this seems to be of a low key compared to the other factors detailed above. The density stratification explained above causes a clear difference in the plankton composition and size structure in the water column and how the large variation in salinity affects different planktonic communities in the present study region is elaborated hereafter.

The autotrophic plankton communities may respond to changes in the nutrient concentrations within a few days, but in the case of heterotrophs, it may take a few weeks to months to respond (Brock et al., 1991; Habeebrehman et al., 2008; Jyothibabu et al., 2010; Karnan et al., 2017a). Therefore, it is rather difficult to track such changes in the present study as we followed a monthly sampling. At the same time, a significant change in the abundance, biomass, size structure and composition of autotrophic and heterotrophic micro-plankton was evident in the data as a response to the hydrographical changes in the study region. Though salinity can restrict phytoplankton to different zones during the SWM, the elevation of nutrients through upwelling and river influx could be assimilated by phytoplankton surviving in these zones (Banse, 1959; Gupta et al., 2016; Karnan et al., 2017a). Even during non-monsoon periods, the estuarine export along the southwest coast is found to support fairly high phytoplankton stock very close to the coastline dominated by comparatively smaller micro-autotrophs (*Skeletonema*, *Odontella*, *Amphiprora*, *Leptocylindrus*, *Pseudo-nitzschia*, *Thalassionema* and *Ceratium*) and diazotrophic cyanobacteria *Trichodesmium* (Gauns et al., 2005; Karnan et al., 2017a).

During the PSWM, micro-heterotrophs live abundantly in the water column as their preferred foods (autotrophic and heterotrophic nano-flagellates) occur in plenty in the water column (Donald et al., 1997; Gauns et al., 2005; Jyothibabu et al., 2006). As the upwelled waters in the nearshore waters originate from ~80-150m depth in the ocean, the dissolved oxygen it carries would be much lower than the surface waters (Gupta et al., 2016). The regions along the southwest coast of India where freshwater capping effect is absent, upwelled water mass comes to the surface, touching the shoreline (Gireeshkumar et al., 2017; Karnan et al., 2017a). In the present case, the increased freshwater flow from the adjacent estuary during SWM inhibited the upwelling of hypoxic water, which could impart stress on organisms living in the bottom (Judkins, 1980; Levin, 2003; Stramma et al., 2012; Gallo

and Levin, 2017; Jyothibabu et al., 2018b). In the present study, the abundance of microheterotrophs was low in the subsurface during the upwelling period, possibly as the result of the stress caused by hypoxia. It was observed earlier that the abundance of heterotrophs increases when hypoxia recedes from the region (Anjusha et al., 2018b). While hypoxia can affect the metazoans in the microzooplankton community, protozoans in the community may not significantly get affected (Gowing et al., 2003). It was noticed elsewhere that protistan micro-zooplankton can efficiently consume heterotrophic nano-flagellates in oxygen deficient upwelling environment (Calbet, 2008).

During the SWM, surface and bottom waters have higher abundance of phytoplankton than in the mid-water, which could be the result of specific phytoplankton communities in different depth zones utilizing the optimum environmental conditions prevailing there. Salinity and PAR are the two major factors controlling the large chain forming diatoms (*Fragilaria* sp., and *Thalassiosira* sp.) in the bottom waters and smaller diatoms (*Thalassionema* sp., and *Skeletonema* sp.) in the surface waters (Anjusha et al., 2018a). During the SWM, though chlorophyll was found high in the surface, the larger sized autotrophs in the sub-surface caused more autotrophic biomass. This implies that a mere calculation of cell abundance or chlorophyll concentration might misrepresent the actual carbon biomass in autotrophs present in different water masses and in this context, the present approach of considering the plankton size and biovolume could be a more realistic approach.

It was noticed that the growth rate of larger phytoplankton (*Fragilaria* sp., *Thalassiosira* sp. and *Coscinodiscus* sp.) increases during nutrient enriched and optimized light conditions (Jyothibabu et al., 2018). Also our recent study support the view that high abundance of spherical/disc-shaped autotrophs occur in the inshore waters along the southwest coast of India during the SWM season mainly associated with the addition of new nutrients to the shelf waters through intensive coastal upwelling process (Karnan et al., 2017a). Recent FlowCAM studies showed that nutrient-rich seawater promote the dominance of spherical and large chain forming diatoms in upwelling regions (Karnan et al., 2017a,b). It was realized in those studies that light condition in the subsurface could be another reason for the increased growth of spherical and large chain forming diatoms. But in the present study, though nutrients were there in the surface waters through river influx, it could mostly support the smaller needle shaped phytoplankton. Dominance of needle shaped phytoplankton is a characteristic feature of the adjacent Cochin backwaters (Madhu et al., 2010; Karnan et al., 2019). Hence the dominance of needle shaped phytoplankton in the surface waters of the present sampling region can directly be attributed to the advected estuarine waters in the region. Many past studies have presented the idea that smaller sized phytoplankton contribute the major part of the autotrophic community during the PSWM and the NEM, leading to a relatively longer microbial food web with

low trophic transfer efficiency (Sieburth et al., 1978; Johnson and Sieburth, 1979; Azam et al., 1983; Banse et al., 1996; Cermeno et al., 2006; Jyothibabu et al., 2008; Ashadevi et al., 2010). During the SWM, larger diatoms dominates and form blooms in the SEAS (Nair and Subrahmanyam, 1955; Nair et al., 1992; Banse et al., 1996; Landry et al., 1998; Karnan et al., 2017a). It was noticed that blooms of large chain forming diatom *Fragilaria* sp., are crucial in sustaining large stocks of Indian oil sardine (Nair and Subrahmanyam, 1955; Preetha, 2015). The large-sized autotrophs during the SWM could be directly grazed upon by smaller fishes and, thus, facilitate the transfer the primary biomass to higher trophic levels through a short food chain (Cushing, 1989; Mann, 1993). Studies have also showed that the upwelling hypoxic waters concentrate shoals of fishes to the surface waters along the southwest coast of India (Banse, 1968; Karnan et al., 2017a, b). The scenario seems slightly different in the present study region, where surface water is low saline and oxygenated, while the subsurface waters is high saline and hypoxic (Figure 11b). In such conditions, the demersal fishes may move away from the hypoxic bottom layers (Banse, 1968; Reghunathan et al., 1984; Rabalais and Turner, 2001; Karnan et al., 2017a) and may try to occupy the surface layers, but there the low salinity of the water may act as another stress. Based on the above aspects, it is proposed on a general perspective that the marine fishery resources availability in the present study area could be constrained by the incursion of hypoxic waters in the bottom and freshwater influx in the surface. The marine pelagic fishes may eventually move away from the coast and may probably aggregate along the edges of these salinity fronts (Figure 11). Not ignoring the possibility that some pelagic fishes (hypotonic) can survive in low saline waters by controlling their osmotic variations but they too get seriously impacted, when the osmotic pressure exceeds the tolerance level (Evans, 1980). It is noticed that long osmotic variation has the potential to affect the reproduction as well as larval development of fishes and other animals (Dolomatov et al., 2012). Factual that more specific studies are required to understand the ecological response of pelagic fishes to habitat compression in the study area due to hypoxia and freshwater influx.

#### **4.5. Conclusion**

This study was carried out to understand the microplankton size structure and composition with respect to the seasonal hydrographic changes in the nearshore waters along the south west coast of India. The PSWM was characterized by warmer water, which was completely replaced by the cooler nutrient-rich water mass during the SWM season. The abundance and biomass of micro-autotrophs were mismatched with high abundance and low biomass during PSWM and low abundance and high biomass during SWM. During the peak SWM, occurrence of two different water masses was evident vertically, one at the surface (warm and less dense) and the other at the subsurface (cool, dense and

oxygen-depleted), which was caused by the freshwater influx at the surface and upwelling in the subsurface. This feature facilitated the dominance of smaller micro-autotrophs in the surface and larger micro-autotrophs in the sub-surface. The present study clearly evidenced that due to temporal changes in water masses in the near-shore waters in the SEAS, there are considerable seasonal and spatial variations in the size structure and composition of the microplankton. Since the source of the surface waters in the study area was the adjacent Cochin backwaters, it supported the dominance of needle shaped smaller phytoplankton. On the other hand, upwelled water in the subsurface promoted the dominance of larger cells. Based on the hydrographical settings in the region, we suggest a habitat compression to fishes especially during the SWM due to the occurrence of hypoxic subsurface and significantly low-saline surface waters.

### **Acknowledgments**

The authors thank the Director of CSIR - National Institute of Oceanography, India and the Scientist in-Charge (CSIR-NIO, Kochi) for facilities and encouragement. We record our sincere thanks to ESSO-INCOIS, India for the funding to CSIR -NIO, Regional Center, Kochi during 2012-2017 under PFZ mission programme. The first author thanks CSIR, India for the fellowship during the period of this work. This is CSIR-NIO contribution.....

### **References**

- Alvarez, E., Lopez-Urrutia, A., Nogueira, E., 2012. Improvement of plankton biovolume estimates derived from image-based automatic sampling devices: application to FlowCAM. *Journal of Plankton Research* 34, 454-469.
- Alvarez, E., Moyano, M., Lopez-Urrutia, A., Nogueira, E., Scharek, R., 2013. Routine determination of plankton community composition and size structure: a comparison between FlowCAM and light microscopy. *Journal of Plankton Research* 36, 170-184.
- Anjusha, A., Jyothibabu, R., Jagadeesan, L., 2018a. Response of microzooplankton community to the hydrographical transformations in the coastal waters off Kochi, along the southwest coast of India. *Continental Shelf Research* 167, 111-124.
- Anjusha, A., Jyothibabu, R., Jagadeesan, L., Savitha, K.M.M., Albin, K.J., 2018b. Seasonal variation of phytoplankton growth and microzooplankton grazing in a tropical coastal water (off Kochi), Southwest coast of India. *Continental Shelf Research* 171, 12-20.
- Ashadevi, C.R., Jyothibabu, R., Sabu, P., Jacob, J., Habeebrehman, H., Prabhakaran, M.P., Jayalakshmi, K.J., Achuthankutty, C.T., 2010. Seasonal variations and trophic ecology of microzooplankton in the southeastern Arabian Sea. *Continental Shelf Research* 30, 1070-1084.
- Azam, F., Fenchel, T., Field, J.G., Gray, J.S., Meyer-Reil, L.A., Thingstad, F., 1983. The ecological role of water-column microbes in the sea. *Marine Ecology Progress Series*. Oldendorf 10, 257-263.

- Banse, K., 1959. On upwelling and bottom-trawling off the southwest coast of India. *Journal of the Marine Biological Association of India* 1, 33-49.
- Banse, K., 1968. Hydrography of the Arabian Sea shelf of India and Pakistan and effects on demersal fishes, *Deep Sea Research and Oceanographic Abstracts*. Elsevier, pp. 45-79.
- Banse, K., 1982. Mass-scaled rates of respiration and intrinsic growth in very small invertebrates. *Marine Ecology Progress Series* 9, 281-297.
- Banse, K., Vijayaraghavan, S., Madhupratap, M., 1996. On the possible causes of the seasonal phytoplankton blooms along the southwest coast of India. *Oceanographic Literature Review* 6, 605-606.
- Becker, R.A., Chambers, J.M., Wilks, A.R., 1988. *The New S Language* Pacific Grove, CA: Wadsworth & Brooks/Cole.
- Bhattathiri, P.M.A., Pant, A., Sawant, S.S., Gauns, M., Matondkar, S.G.P., Mahanraju, R., 1996. Phytoplankton production and chlorophyll distribution in the eastern and central Arabian Sea in 1994-1995. *Current Science* 71, 857-862.
- Brock, J.C., McClain, C.R., Luther, M.E., Hay, W.W., 1991. The phytoplankton bloom in the northwestern Arabian Sea during the southwest monsoon of 1979. *Journal of Geophysical Research: Oceans* (1978-2012) 96, 20623-20642.
- Calbet, A., 2008. The trophic roles of microzooplankton in marine systems. *ICES Journal of Marine Science* 65, 325-331.
- Caromel, A.G.M., Schmidt, D.N., Phillips, J.C., Rayfield, E.J., 2014. Hydrodynamic constraints on the evolution and ecology of planktic foraminifera. *Marine Micropaleontology* 106, 69-78.
- Cermeno, P., Maranon, E., Perez, V., Serret, P., Fernandez, E., Castro, C.G., 2006. Phytoplankton size structure and primary production in a highly dynamic coastal ecosystem (Ria de Vigo, NW-Spain): Seasonal and short-time scale variability. *Estuarine, Coastal and Shelf Science* 67, 251-266.
- Chambers, J.M., Hastie, T.J., 1992. *Statistical models in S*. Wadsworth & Brooks/Cole Advanced Books & Software Pacific Grove, CA.
- Cushing, D.H., 1989. A difference in structure between ecosystems in strongly stratified waters and in those that are only weakly stratified. *Journal of Plankton Research* 11, 1-13.
- De Sousa, S.N., Kumar, M.D., Sardesai, S., Sarma, V., 1996. Seasonal variability in oxygen and nutrients in. *Current science* 71, 847-851.
- Dolomatov, S.I., Zukow, W., Novikov, N.Y., Muszkieta, R., Bulatowicz, I., Dzierzanowski, M., Kazmierczak, U., Strojek, K., 2012. The regulation of osmotic and ionic balance in fish reproduction and in the early stages of ontogeny. *Russian Journal of Marine Biology* 38, 365-374.
- Donald, K.M., Scanlan, D.J., Carr, N.G., Mann, N.H., Joint, I., 1997. Comparative phosphorus nutrition of the marine cyanobacterium *Synechococcus* WH7803 and the marine diatom *Thalassiosira weissflogii*. *Journal of Plankton Research* 19, 1793-1813.



- Evans, D.H., 1980. Osmotic and Ionic Regulation by Freshwater and Marine Fishes. , in: Ali, M.A. (Ed.), *Environmental Physiology of Fishes*. NATO Advanced Study Institutes Series (Series A: Life Science). Springer, Boston, MA, pp. 93-122.
- Friendly, M., 2002. Corrgrams: Exploratory displays for correlation matrices. *The American Statistician* 56, 316-324.
- Gallo, N.D., Levin, L.A., 2016. Fish ecology and evolution in the world's oxygen minimum zones and implications of ocean deoxygenation, *Advances in Marine Biology*. Elsevier, pp. 117-198.
- Gauns, M., Madhuratap, M., Ramaiah, N., Jyothibabu, R., Fernandes, V., Paul, J.T., Kumar, S.P., 2005. Comparative accounts of biological productivity characteristics and estimates of carbon fluxes in the Arabian Sea and the Bay of Bengal. *Deep Sea Research Part II: Topical Studies in Oceanography* 52, 2003-2017.
- Gireeshkumar, T.R., Mathew, D., Pratihary, A.K., Naik, H., Narvekar, K.U., Araujo, J., Balachandran, K.K., Muraleedharan, K.R., Thorat, B., Nair, M., 2017. Influence of upwelling induced near shore hypoxia on the Alappuzha mud banks, South West Coast of India. *Continental Shelf Research* 139, 1-8.
- Gowing, M.M., Garrison, D.L., Wishner, K.F., Gelfman, C., 2003. Mesopelagic microplankton of the Arabian Sea. *Deep Sea Research Part I: Oceanographic Research Papers* 50, 1205-1234.
- Grasshoff, K., Ehrhardt, M., Kremling, K., 1983. *Methods of Seawater Analysis* (Eds.). Verlag Chemie, Weinheim, 89–224.
- Gupta, G.V.M., Sudheesh, V., Sudharma, K.V., Saravanane, N., Dhanya, V., Dhanya, K.R., Lakshmi, G., Sudhakar, M., Naqvi, S.W.A., 2016. Evolution to decay of upwelling and associated biogeochemistry over the southeastern Arabian Sea shelf. *Journal of Geophysical Research: Biogeosciences* 121, 159-175.
- Habeebrehman, H., Prabhakaran, M.P., Jacob, J., Sabu, P., Jayalakshmi, K.J., Achuthankutty, C.T., Revichandran, C., 2008. Variability in biological responses influenced by upwelling events in the Eastern Arabian Sea. *Journal of Marine Systems* 74, 545-560.
- Hareeshkumar, P.V., Anand,P., 2016. Coastal upwelling of the southwest cost of India: observations and simulations. *International Journal of Digital Earth* 9, 1256-1274.
- Johnson, P.W., Sieburth, J.M., 1979. Chroococcoid cyanobacteria in the sea: A ubiquitous and diverse phototrophic biomass. *Limnology and Oceanography* 24, 928-935.
- Judkins, D.C., 1980. Vertical distribution of zooplankton in relation to the oxygen minimum off Peru. *Deep Sea Research Part A. Oceanographic Research Papers* 27, 475-487.
- Jyothibabu, R., Balachandran, K.K., Jagadeesan, L., Karnan, C., Arunpandi, N., Naqvi, S.W.A., Pandiyarajan, R.S., 2018a. Mud Banks along the southwest coast of India are not too muddy for plankton. *Scientific Reports* 8, 2544.
- Jyothibabu, R., Devi, C.R.A., Madhu, N.V., Sabu, P., Jayalakshmy, K.V., Jacob, J., Habeebrehman, H., Prabhakaran, M.P., Balasubramanian, T., Nair, K.K.C., 2008. The response of microzooplankton (20-200µm) to coastal upwelling and summer stratification in the southeastern Arabian Sea. *Continental Shelf Research* 28, 653-671.

- Jyothibabu, R., Jagadeesan, L., Karnan, C., Arunpandi, N., Pandiyarajan, R.S., Balachandran, K.K., 2018b. Ecological indications of copepods to oxygen-deficient near-shore waters. *Ecological Indicators* 93, 76-90.
- Jyothibabu, R., Madhu, N.V., Habeebrehman, H., Jayalakshmy, K.V., Nair, K.K.C., Achuthankutty, C.T., 2010. Re-evaluation of 'paradox of mesozooplankton' in the eastern Arabian Sea based on ship and satellite observations. *Journal of Marine Systems* 81, 235-251.
- Jyothibabu, R., Madhu, N.V., Jayalakshmi, K.V., Balachandran, K.K., Shiyas, C.A., Martin, G.D., Nair, K.K.C., 2006. Impact of freshwater influx on microzooplankton mediated food web in a tropical estuary (Cochin backwaters-India). *Estuarine, Coastal and Shelf Science* 69, 505-518.
- Karnan, C., Jyothibabu, R., Arunpandi, N., Jagadeesan, L., Muraleedharan, K.R., Pratihari, A.K., Balachandran, K.K., Naqvi, S.W.A., 2017a. Discriminating the biophysical impacts of coastal upwelling and mud banks along the southwest coast of India. *Journal of Marine Systems* 172, 24-42.
- Karnan, C., Jyothibabu, R., Kumar, T.M.M., Balachandran, K.K., Arunpandi, N., Jagadeesan, L., 2017b. Seasonality in Autotrophic Mesoplankton in a Coastal Upwelling-mud bank Environment along the Southwest Coast of India and its Ecological Implications. *Continental Shelf Research* 146, 1-12.
- Karnan, C., Jyothibabu, R., Manoj Kumar, T.M., Arunpandi, N., Jagadeesan, L., 2017c. On the Accuracy of Assessing Copepod Size and Biovolume using FlowCAM and Traditional Microscopy. *Indian Journal of Geo Marine Systems* 46, 1261-1264.
- Karp-Boss, L., Boss, E., 2016. The elongated, the squat and the spherical: selective pressures for phytoplankton shape, in: Glibert, P.M., Kana, T.M. (Eds.), *Aquatic microbial ecology and biogeochemistry: a dual perspective*. Springer, pp. 25-34.
- Krishnakumar, K.N., Rao, G.P., Gopakumar, C.S., 2009. Rainfall trends in twentieth century over Kerala, India. *Atmospheric Environment* 43, 1940-1944.
- Landry, M.R., Brown, S.L., Campbell, L., Constantinou, J., Liu, H., 1998. Spatial patterns in phytoplankton growth and microzooplankton grazing in the Arabian Sea during monsoon forcing. *Deep Sea Research Part II: Topical Studies in Oceanography* 45, 2353-2368.
- Leps, J., Smilauer, P., 2003. *Multivariate analysis of ecological data using CANOCO*. Cambridge University Press.
- Levin, L., 2003. Oxygen minimum zone benthos: adaptation and community response to hypoxia. *Oceanography and Marine Biology* 41, 1-45.
- Madhu, N. V., Balachandran, K. K., Martin, G. D., Jyothibabu, R., Thottathil, S. D., Nair, M., Joseph, T., Kusum, K. K. (2010). Short-term variability of water quality and its implications on phytoplankton production in a tropical estuary (Cochin backwaters—India). *Environmental Monitoring and Assessment*, 170(1-4), 287-300.
- Madhupratap, M., Kumar, S.P., Bhattathiri, P.M.A., Kumar, M.D., Raghukumar, S., Nair, K.K.C., Ramaiah, N., 1996. Mechanism of the biological response to winter cooling in the northeastern Arabian Sea. *Nature* 384, 549-552.

- Madhupratap, M., Nair, S.R.S., Haridas, P., Padmavati, G., 1990. Response of zooplankton to physical changes in the environment: coastal upwelling along the central west coast of India. *Journal of Coastal Research*, 413-426.
- Mann, K.H., 1993. Physical oceanography, food chains, and fish stocks: a review. *ICES Journal of Marine Science: Journal du Conseil* 50, 105-119.
- Marquis, E., Niquil, N., Dupuy, C., 2011. Does the study of microzooplankton community size structure effectively define their dynamics? Investigation in the Bay of Biscay (France). *Journal of Plankton Research* 33, 1104-1118.
- Marshall, S.M., 1973. Respiration and feeding in copepods. *Advanced Marine Biology* 11, 57-120.
- Menden-Deuer, S., Lessard, E.J., 2000. Carbon to volume relationships for dinoflagellates, diatoms, and other protist plankton. *Limnology and Oceanography* 45, 569-579.
- Michaels, A.F., Caron, D.A., Swanberg, N.R., Howse, F.A., Michaels, C.M., 1995. Planktonic sarcodines (Acantharia, Radiolaria, Foraminifera) in surface waters near Bermuda: abundance, biomass and vertical flux. *Journal of Plankton Research* 17, 131-163.
- Muraleedharan, P.M., Prasanna Kumar, S., 1996. Arabian Sea upwelling-A comparison between coastal and open ocean regions. *Current Science* 71, 842-846.
- Nair, R.V., Subrahmanyam, R., 1955. The diatom, *Fragilaria oceanica* Cleve, an indicator of abundance of the Indian oil sardine, *Sardinella longiceps* Cuv. and Val. *Current Science* 24, 41-42.
- Nair, S.R.S., Devassy, V.P., Madhupratap, M., 1992. Blooms of phytoplankton along the west coast of India associated with nutrient enrichment and the response of zooplankton. *Science of the Total Environment*, 819-828.
- Narayanan, S., Kottayil, A., Mohanakumar, K., 2016. Monsoon low-level jet over the gateway of Indian summer monsoon: a comparative study for two distinct monsoon years. *Meteorology and Atmospheric Physics* 128, 689-696.
- Olson, E., 2011a. Particle shape factors and their use in image analysis part 1: theory. *Journal of GXP Compliance* 15, 85-96.
- Olson, E., 2011b. Particle shape factors and their use in image analysis part II: practical applications. *Journal of GXP Compliance* 15, 77.
- Pomeroy, L.R., leB. Williams, P.J., Azam, F., Hobbie, J.E., 2007. The microbial loop. *Oceanography* 20, 28-33.
- Preetha, G.N., 2015. Studies on major small pelagic fishes along the Kerala Coast with respect to the Potential Fishery Zone (PFZ) advisories (Ph.D. Thesis). Central Marine Fisheries Research Institute, Cochin, India, p. 172.
- Qasim, S.Z., 1982. Oceanography of the northern Arabian Sea. *Deep Sea Research Part A. Oceanographic Research Papers* 29, 1041-1068.
- R Core Team (2018). R: A language and environment for statistical computing. R Foundation for Statistical Computing, Vienna, Austria. <https://www.R-project.org/>.

- Rabalais, N.N., Turner, R.E., 2001. Coastal hypoxia: consequences for living resources and ecosystems. American Geophysical Union, Washington, D.C.
- Ramamirtham, C., Jayaraman, R., 1960. Hydrographical features of the continental shelf waters off Cochin during the years 1958 and 1959. *Journal of the Marine Biological Association of India* 2, 199-207.
- Ramamirtham, C., Jayaraman, R., 1963. Some aspects of the hydrographical conditions of the backwaters around Willingdon Island (Cochin). *Journal of the Marine Biological Association of India* 5, 170-177.
- Regunathan, A., Gopinathan, C.P., Mathew, K.J., Rao, D.S., Murty, A.V.S., 1984. Ecology of mudbanks-Benthos. *CMFRI Bulletin* 31, 40-45.
- Royston, P., 1995. Remark AS R94: A remark on algorithm AS 181: The W-test for normality. *Journal of the Royal Statistical Society. Series C (Applied Statistics)* 44, 547-551.
- Sanilkumar, K.V., Kumar, P.V.H., Joseph, J., Panigrahi, J.K., 2004. Arabian Sea mini warm pool during May 2000. *Current Science* 86, 180-184.
- Shankar, D., Shetye, S.R., 1997. On the dynamics of the Lakshwadeep high and low in the southeastern Arabian Sea. *Journal of Geophysical Research* 102, 12551-12562.
- Shenoi, S.S.C., Shankar, D., Gopalakrishna, V.V., Durand, F., 2005. Role of ocean in the genesis and annihilation of the core of the warm pool in the southeastern Arabian Sea. *Mausam* 56, 147-160.
- Sieburth, J.M., Smetacek, V., Lenz, J.r., 1978. Pelagic ecosystem structure: heterotrophic compartments of the plankton and their relationship to plankton size fractions. *Limnology and oceanography* 23, 1256-1263.
- Sieracki, C.K., Sieracki, M.E., Yentsch, C.S., 1998. An imaging-in-flow system for automated analysis of marine microplankton. *Marine Ecology Progress Series* 168, 285-296.
- Simon, A., Mohankumar, K., 2004. Spatial variability and rainfall characteristics of Kerala. *Journal of Earth System Science* 113, 211-221.
- Smitha, B.R., Sanjeevan, V.N., Vimalkumar, K.G., Revichandran, C., 2008. On the upwelling off the southern tip and along the west coast of India. *Journal of Coastal Research* 24, 95-102.
- Stramma, L., Prince, E.D., Schmidtko, S., Luo, J., Hoolihan, J.P., Visbeck, M., Wallace, D.W.R., Brandt, P., Kortzinger, A., 2012. Expansion of oxygen minimum zones may reduce available habitat for tropical pelagic fishes. *Nature Climate Change* 2, 33.
- Subrahmanyam, R., 1959. Studies on the phytoplankton of the west coast of india. *Proceedings of the Indian Academy of Science, Part I*, 508, 113-187.
- Tada, K., Pithakpol, S., Yano, R., Montani, S., 2000. Carbon and nitrogen content of *Noctiluca scintillans* in the Seto Inland Sea, Japan. *Journal of Plankton Research* 22, 1203-1211.
- Verity, P.G., Lagdon, C., 1984. Relationships between lorica volume, carbon, nitrogen, and ATP content of tintinnids in Narragansett Bay. *Journal of Plankton Research* 6, 859-868.

Verity, P.G., Robertson, C.Y., Tronzo, C.R., Andrews, M.G., Nelson, J.R., Sieracki, M.E., 1992. Relationships between cell volume and the carbon and nitrogen content of marine photosynthetic nanoplankton. *Limnology and Oceanography* 37, 1434-1446.

Ward, B.A., Dutkiewicz, S., Jahn, O., Follows, M.J., 2012. A size-structured food-web model for the global ocean. *Limnology and Oceanography* 57, 1877-1891.

Wyrski, K., 1973. Physical oceanography of the Indian Ocean. In 'The Biology of the Indian Ocean'. (Eds B. Zeitzschel and SA Gerlach.) pp. 18-36. Springer-Verlag: Berlin.

Yandell, B., 1997. Practical data analysis for designed experiments. Routledge, New York.

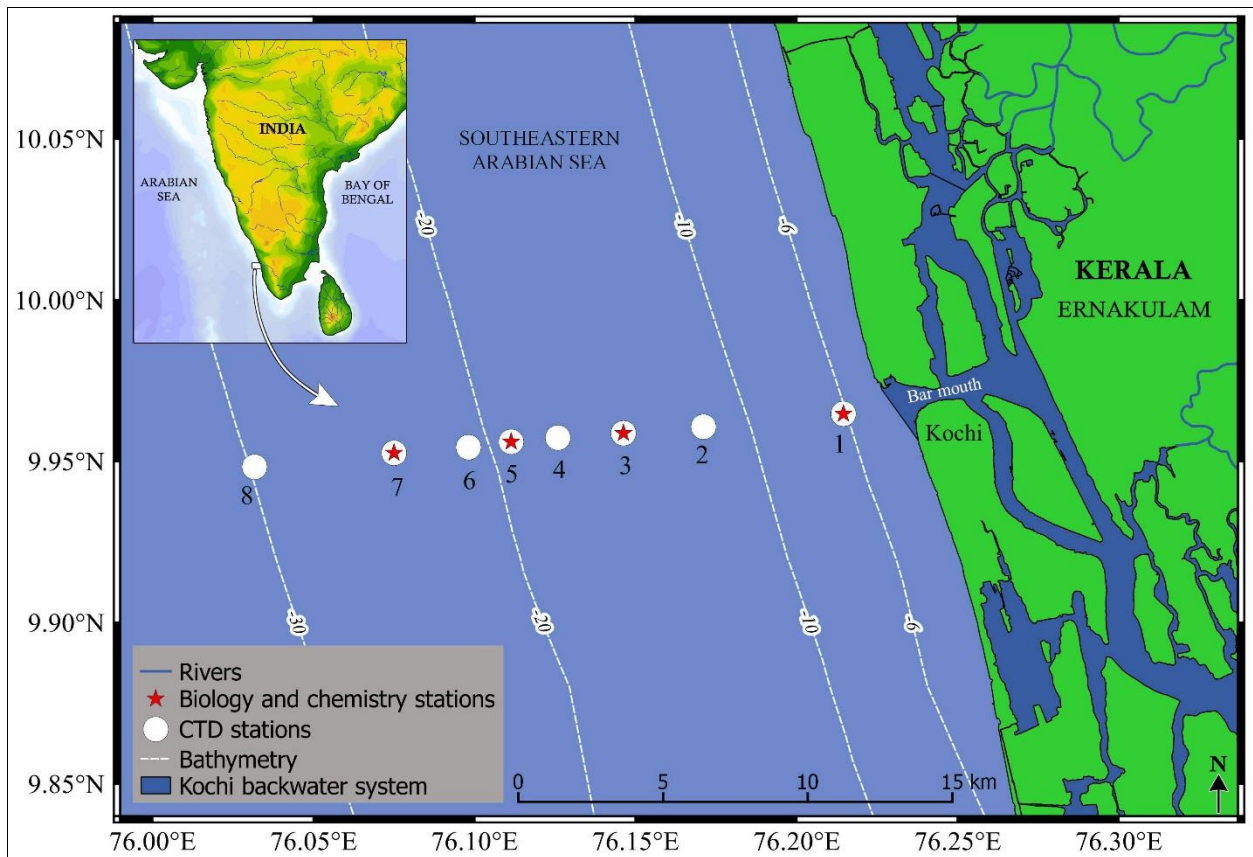


**Figure 1** - Sampling locations along the cross-shore transect off Kochi in the South-Eastern Arabian Sea. Sampling locations were distributed up to 30m depth in the nearshore waters off Kochi. CTD was operated in all the locations (1 - 8), whereas, water samples for chemical and micro-plankton analyses were collected from four selected locations (1, 3, 5, and 7) using a Niskin sampler.

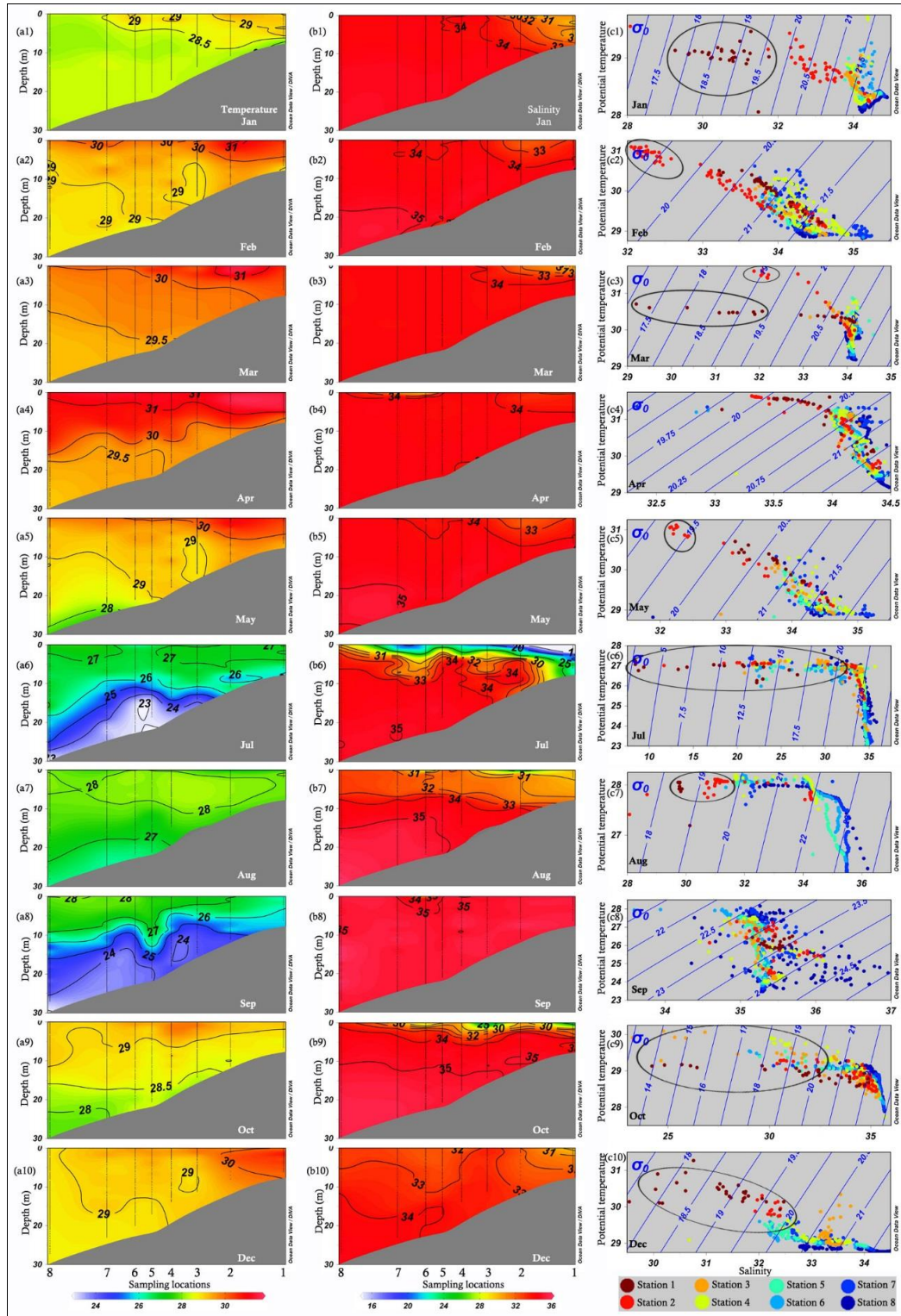


**Figure 2** - Monthly vertical distribution of (a1-a10) temperature ( $^{\circ}\text{C}$ ), (b1-b10) salinity along the cross-shore transect off Kochi. Panel (c1-c10) represents month-wise temperature - salinity (T-S) diagram marked with strong vertical gradients (stratification). No data in June and November.

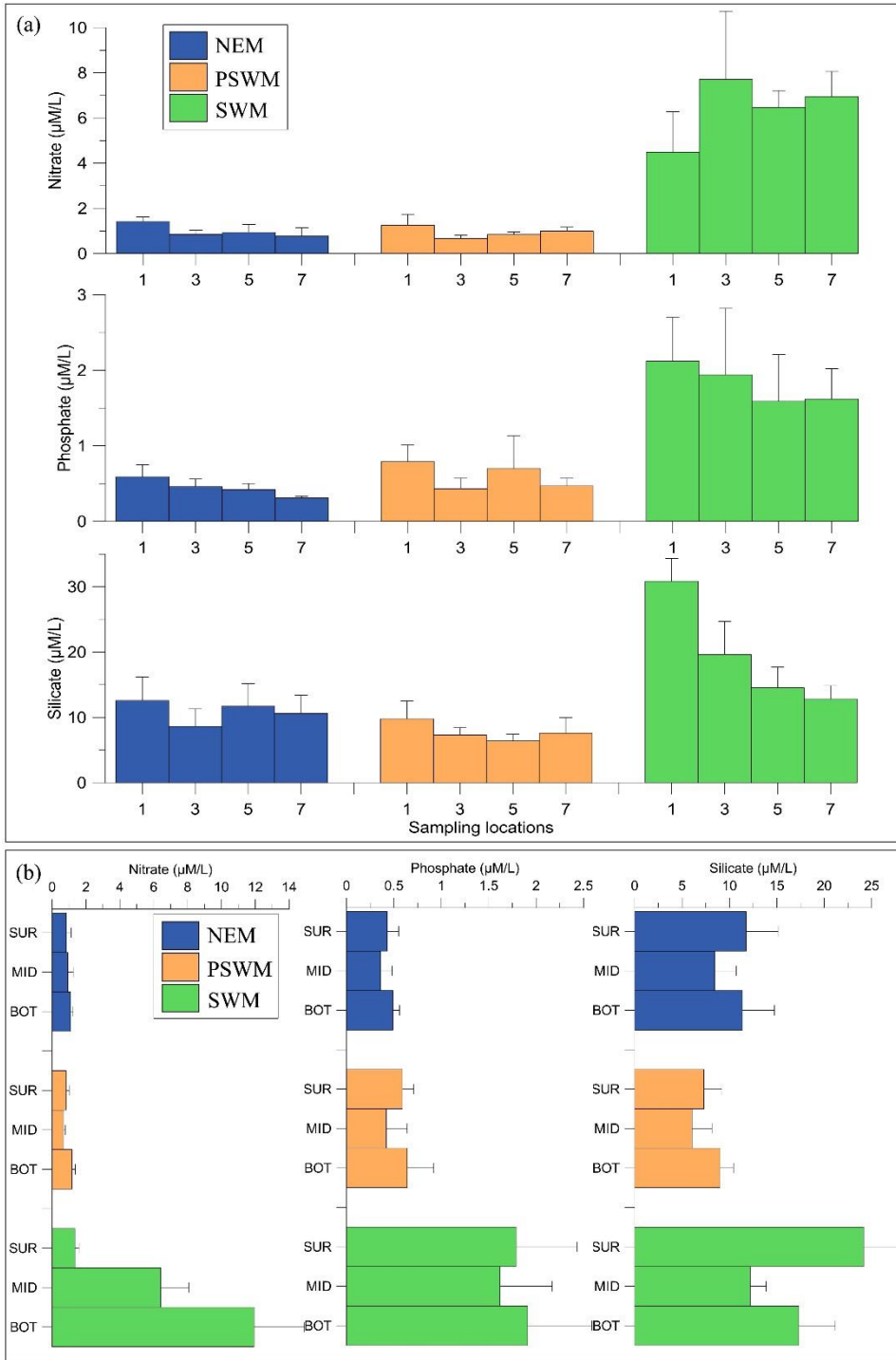


**Figure 3** - The distribution of major nutrients (nitrate, phosphate and silicate) in the study region (a) spatial variation during different seasons, (b) seasonal variation in different discrete depths. Error bars indicate standard error.

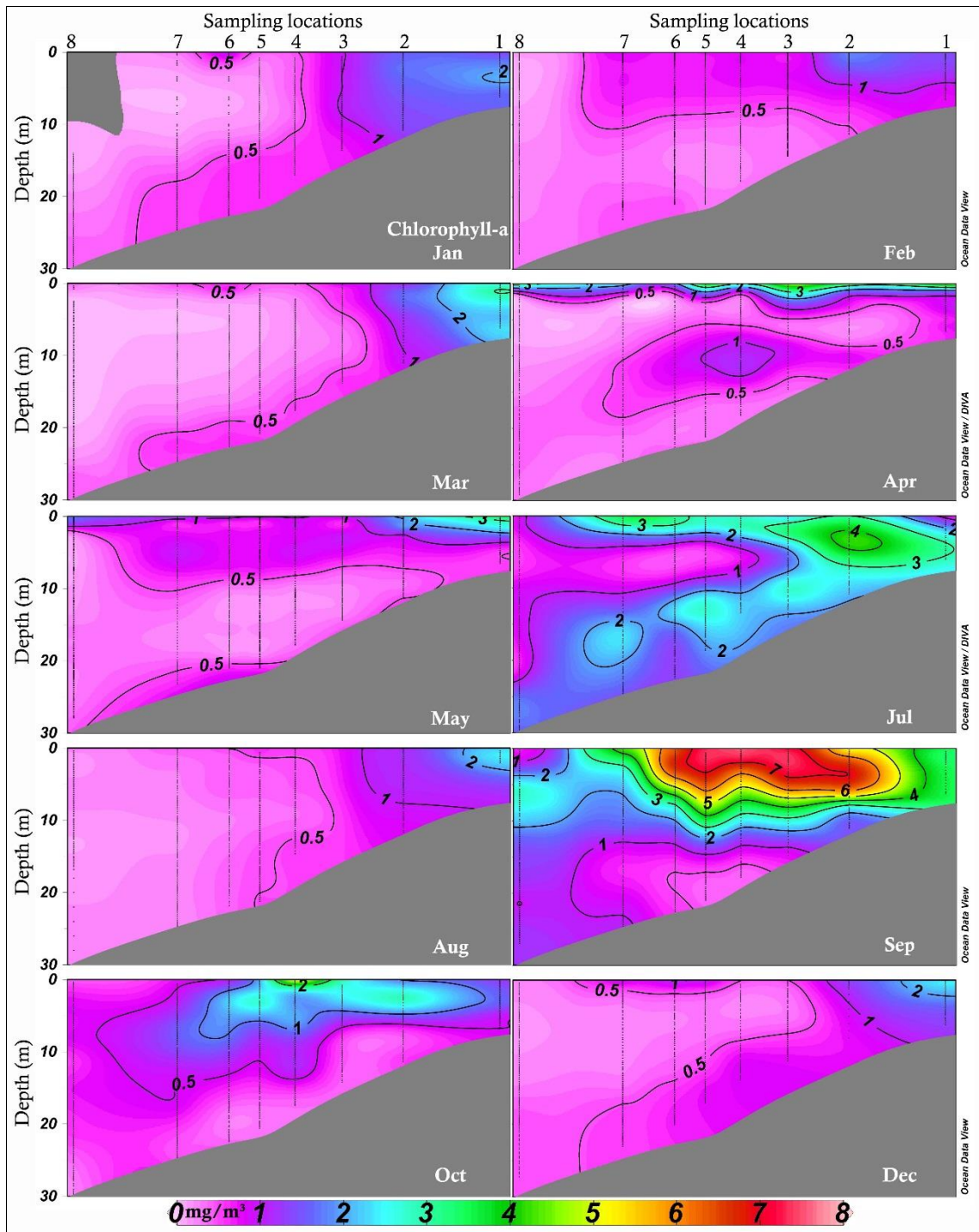


**Figure 4** - Monthly time series of chlorophyll *a* (mg/m<sup>3</sup>) in colour gradients. No data represented for June and November.



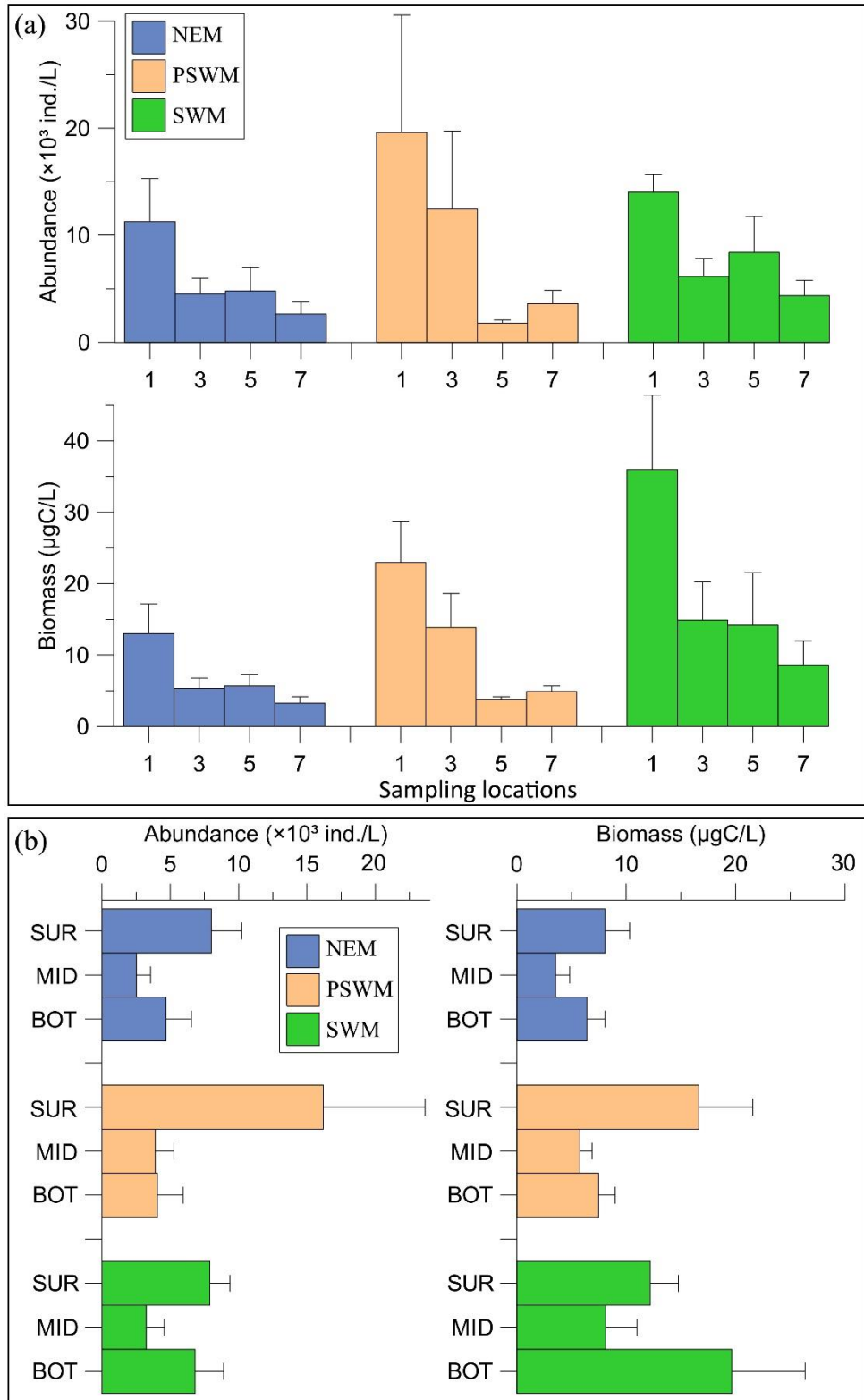


**Figure 5** - Seasonality of autotrophic microplankton abundance and biomass (a) spatial variation during different seasons, (b) seasonal variation in different discrete depths. Error bars indicate standard error.

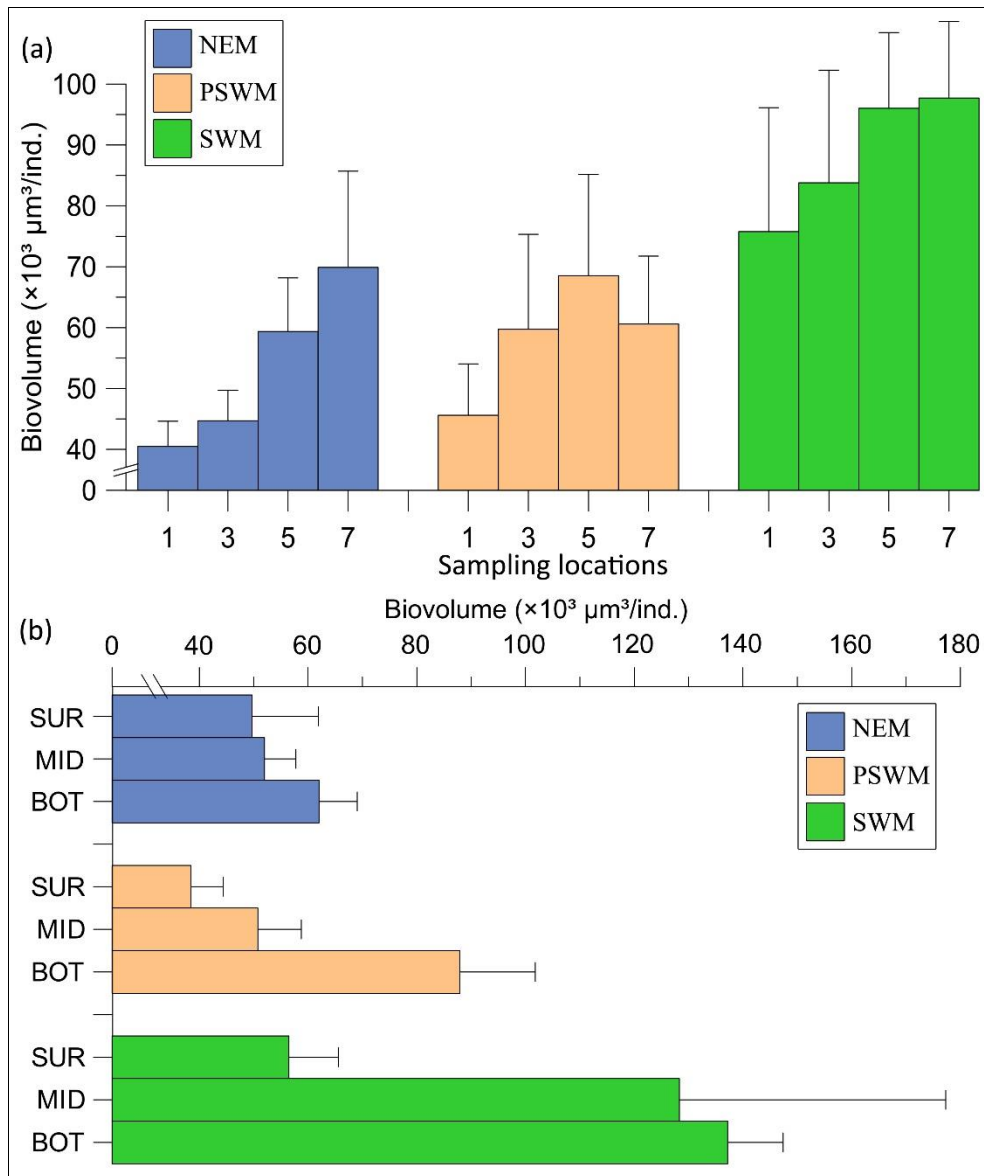


**Figure 6** - Mean biovolume of autotrophic microplankton (a) spatial variation during different seasons, (b) seasonal variation in different discrete depths. Error bars indicate standard error.

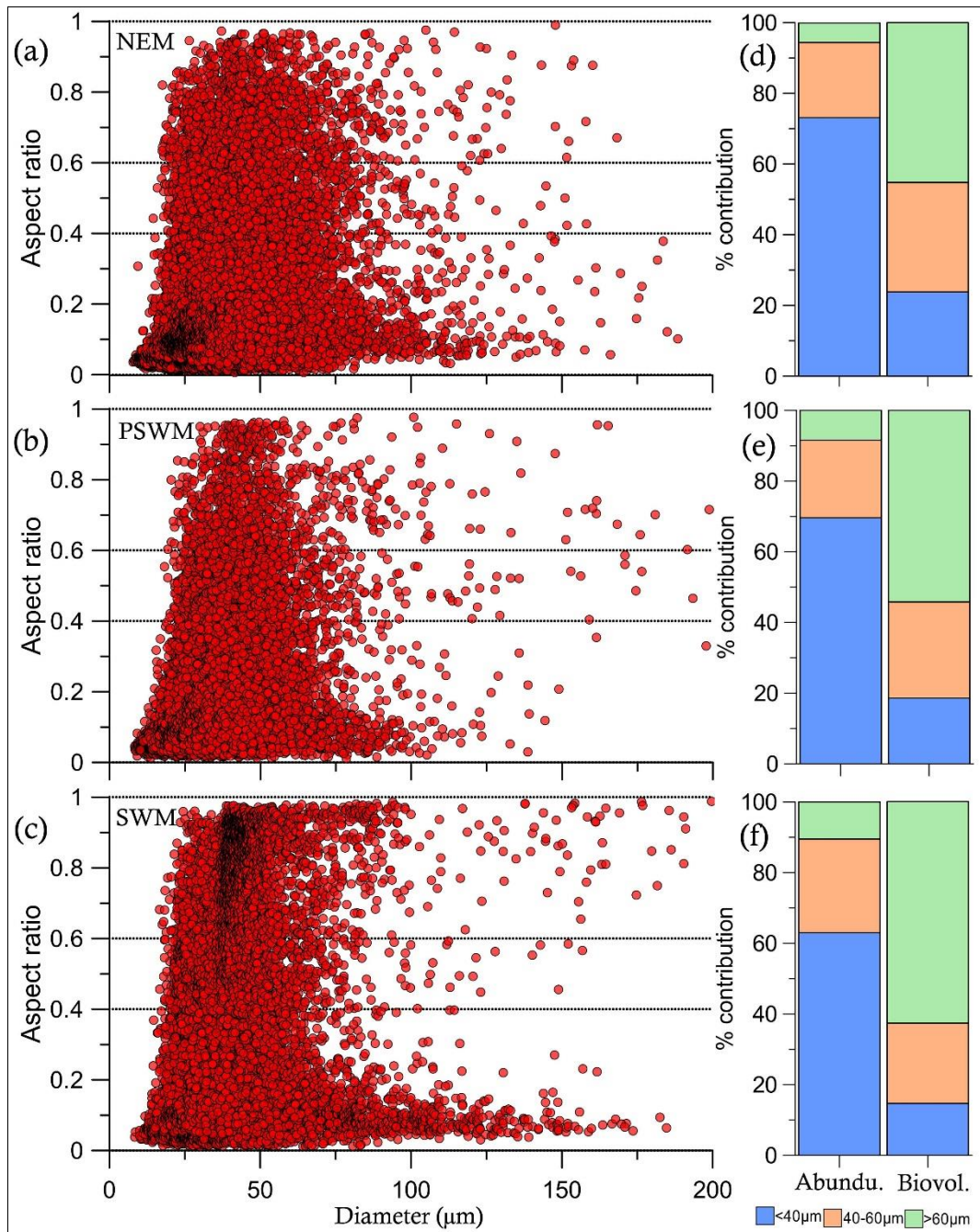


**Figure 7** - The size of autotrophs (diameter) with respect to their shape (aspect ratio) during (a) NEM, (b) PSWM and (c) SWM. The aspect ratio towards 0 represents needle shape (<0.4) and towards 1 represents spherical shape (>0.6). Throughout the year, needle shaped plankton dominate in abundance. Significant contribution of spherical shaped plankton was found during the SWM. All autotrophs were grouped under three size classes as <40μm (smaller), 40-60μm (medium) and >60μm (larger), and presented for (d) NEM, (e) PSWM and (f) SWM. During all the seasons, smaller autotrophs though found in high number, contributed less to the total biovolume. On the other hand, larger autotrophs though found in less numbers contributed more to the total biovolume. The graphs made with more than 16000 individual size measurements for each season.

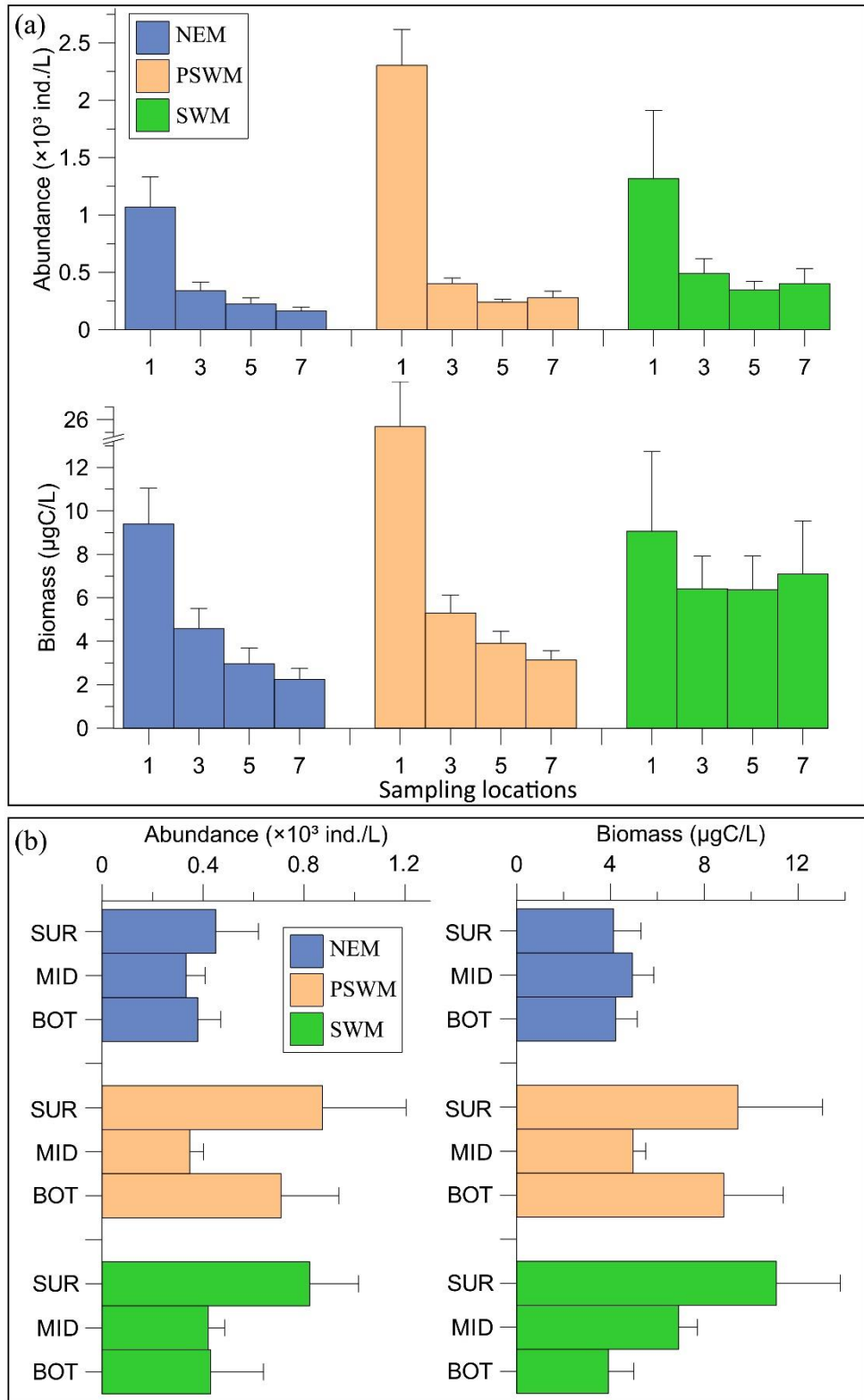


**Figure 8** - Seasonal mean heterotrophic abundance and biomass representing (a) spatial variation during different seasons, (b) seasonal variation in different discrete depths. Error bars indicate standard error.

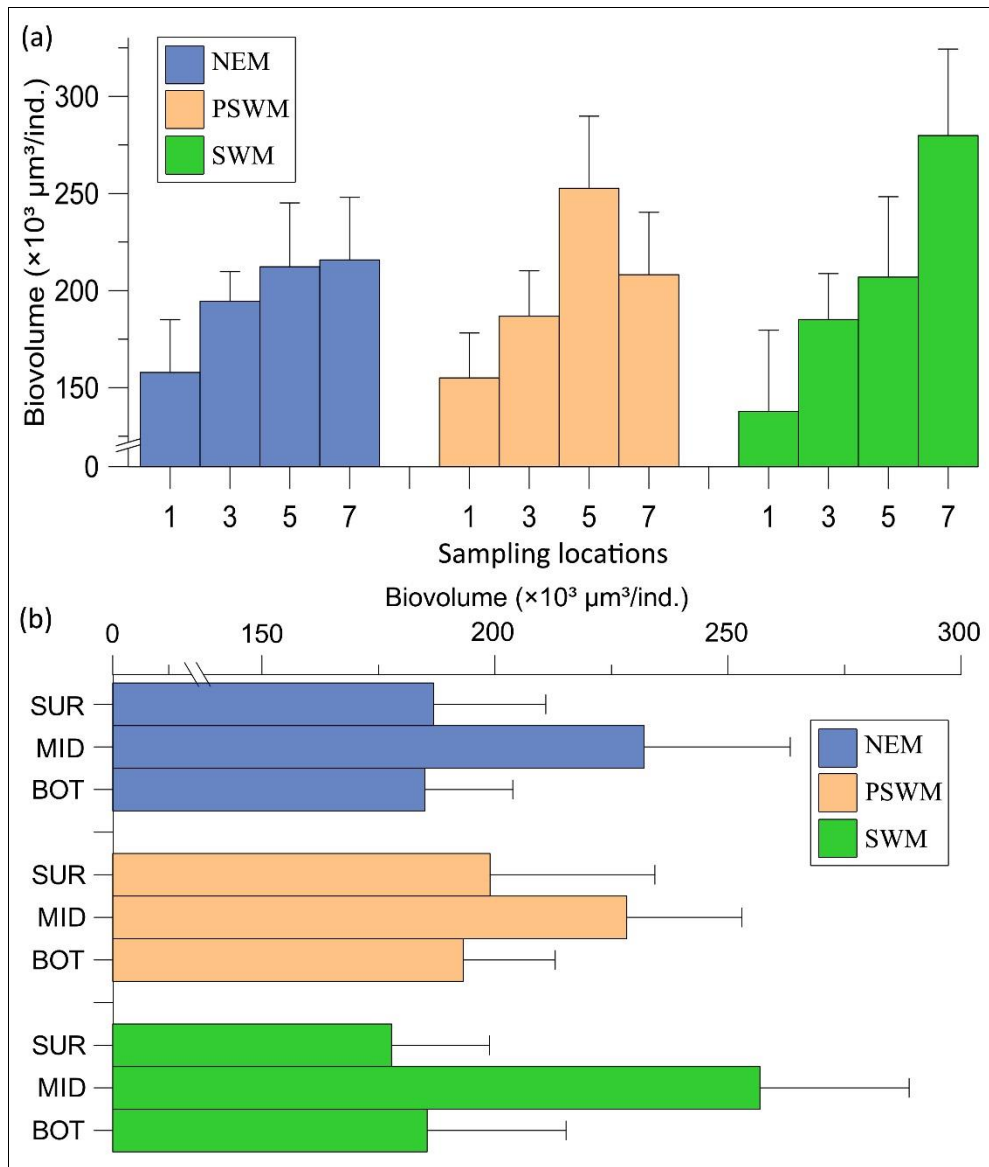


**Figure 9** - Means biovolume of heterotrophic microplankton in (a) spatial variation during different seasons, (b) seasonal variation in different discrete depths.

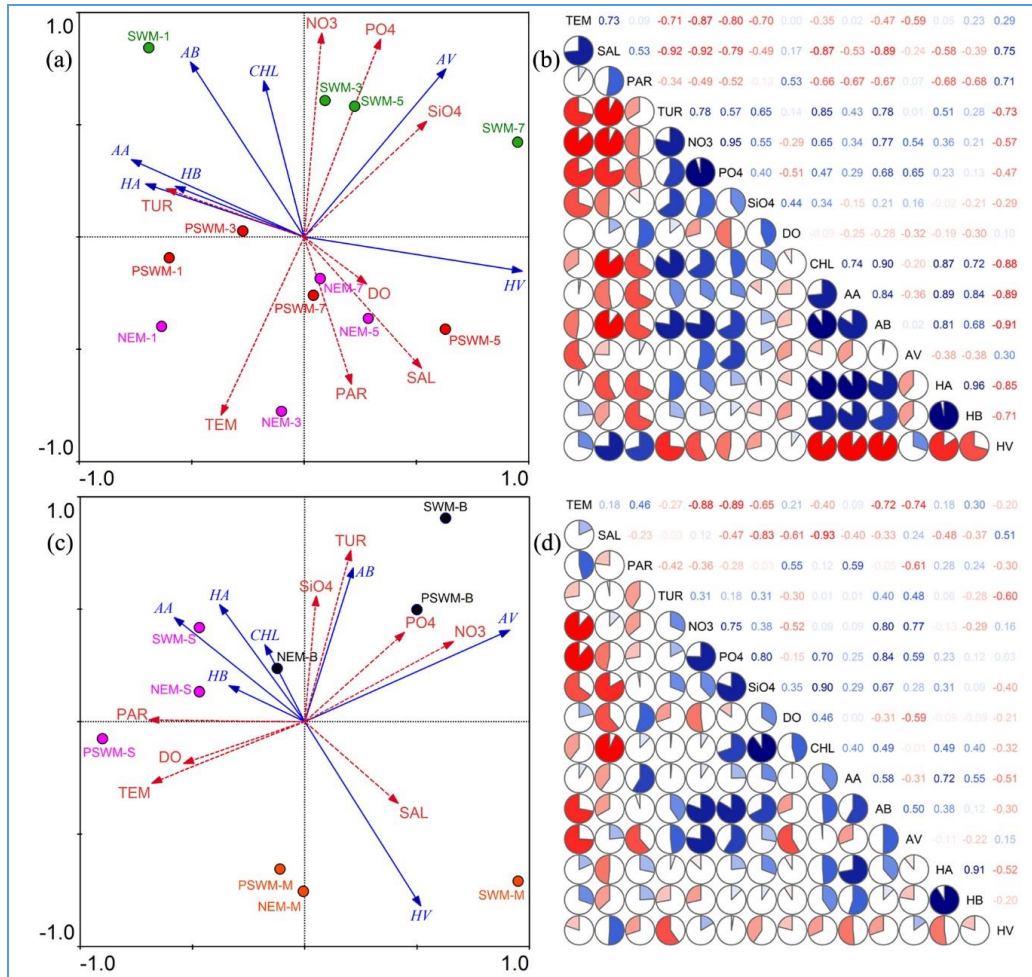


**Figure 10** - The redundancy analysis (RDA) plot and the multivariable correlation plot of various parameters. These analyses results for waters along the transect are presented in (a) and (b) and monthly mean of three discrete depths (surface, mid and bottom) in the water column in (c) and (d). In the left side panels, RDA plots represent sampling locations and depths marked in colour filled dots, physicochemical and biological parameters presented as dashed red and blue arrows, respectively. In the right side panels, the multivariate correlation table presented as correlogram, wherein, lower left diagonal shows pie charts and upper right diagonal shows correlation coefficients. Colour codes red indicates negative and blue indicates positive correlation and the colour intensity represents the strength of the correlation. The significant ( $p < 0.05$ ) correlation coefficient values for waters along the transect is  $> 0.6$  and  $< -0.6$ , and for the water column is  $> 0.7$  and  $< -0.7$ . Abbreviations: NEM - Northeast Monsoon, PSWM - Pre-Southwest Monsoon, SWM - Southwest Monsoon, S - Surface, M - Middle, B - Bottom. 1-7 is the sampling locations from coastal to offshore, TEM - Temperature, SAL - Salinity, PAR - Photosynthetically available radiation, TUR - Turbidity, NO<sub>3</sub> - Nitrate, PO<sub>4</sub> - Phosphate, SiO<sub>4</sub> - Silicate, CHL - Chlorophyll *a*, AA - Autotroph abundance, AB - Autotroph biomass, AV - Autotrophs biovolume, HA - Heterotroph abundance, HB - Heterotroph biomass, HV - Heterotrophs biovolume.

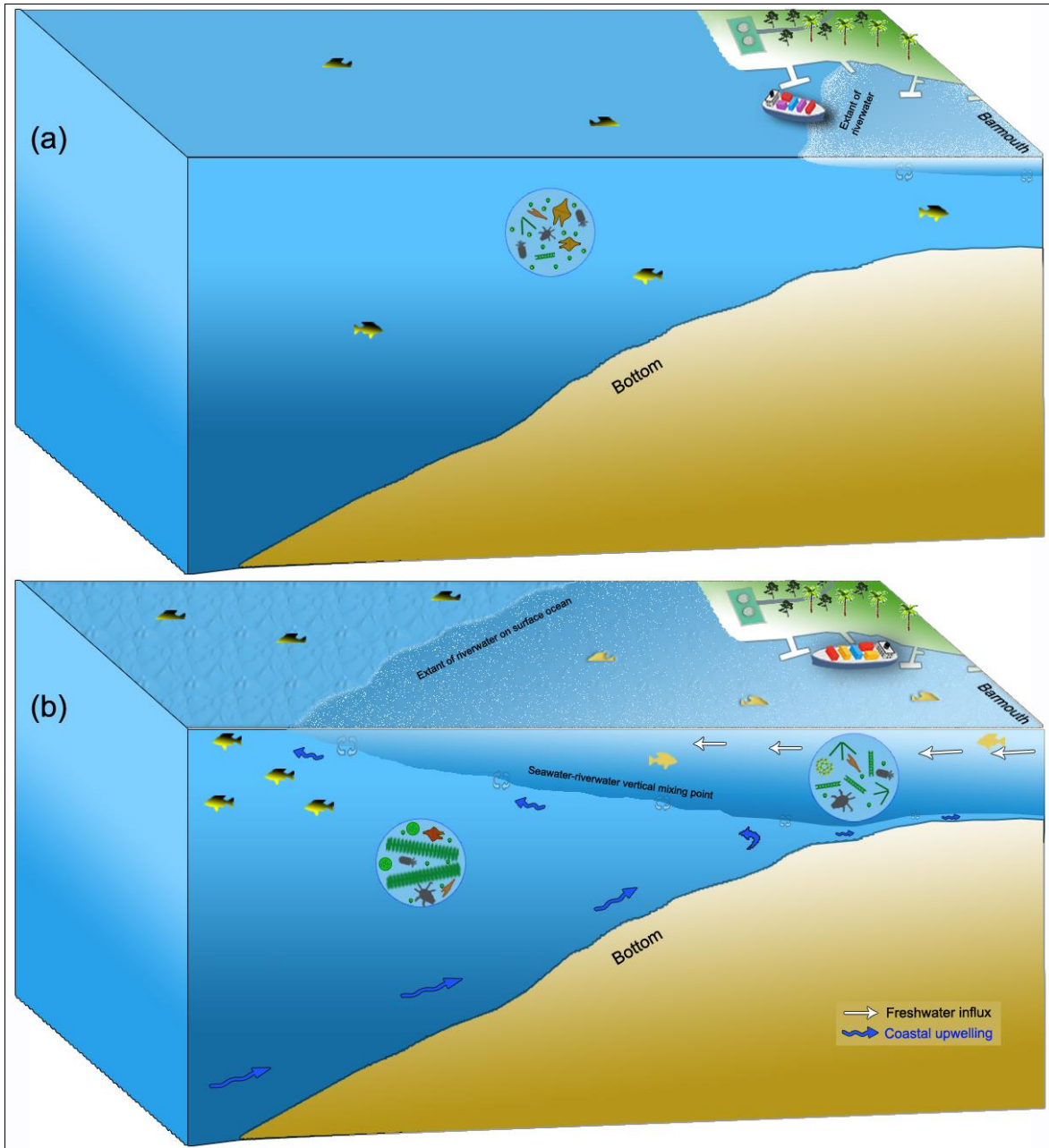


**Figure 11** - Schematic representation of the water column in the sampling domain during (a) non-monsoon period and (b) monsoon period. The high estuarine influx into the nearshore waters during SWM leads to strong vertical zonation, which significantly alters the plankton diversity and size structure in the surface and subsurface waters.

## Tables

	<b>NEM</b>	<b>PSWM</b>	<b>SWM</b>
<b>TEM</b>	29.17 (0.18)	29.96 (0.21)	26.38 (0.43)
<b>SAL</b>	33.67 (0.24)	34.08 (0.14)	32.3 (1.54)
<b>PAR</b>	322 (125)	204 (86)	104 (45)
<b>TUR</b>	3.4 (1.06)	3.08 (0.9)	4.59 (1.26)
<b>NO<sub>3</sub></b>	0.89 (0.15)	0.88 (0.11)	6.56 (1.71)
<b>PO<sub>4</sub></b>	0.38 (0.06)	0.55 (0.11)	1.77 (0.3)
<b>SIO<sub>4</sub></b>	9.94 (2.01)	7.46 (0.95)	17.89 (2.28)
<b>DO</b>	6.88 (0.4)	4.33 (0.44)	5.08 (0.71)
<b>CHL</b>	0.71 (0.11)	0.63 (0.13)	3.2 (1.38)
<b>AA</b>	5310 (1116)	8430 (2927)	7703 (1237)
<b>AB</b>	6.23 (1.1)	10.3 (2)	16.8 (3.5)
<b>AV</b>	54802 (5313)	59801 (6906)	77128 (7625)
<b>HA</b>	392 (702)	670 (148)	577 (129)
<b>HB</b>	4.38 (0.6)	8 (1.6)	7.1 (1.1)
<b>HV</b>	198490 (14031)	204856 (15916)	208318 (20406)

**Table 1** - The seasonal distribution of physico-chemical and biological parameters. Table presented the mean and standard error in parenthesis. Abbreviation: TEM - Temperature, SAL - Salinity, PAR - Photosynthetically available radiation, TUR - Turbidity, NO<sub>3</sub> - Nitrate, PO<sub>4</sub> - Phosphate, SiO<sub>4</sub> - Silicate, DO - Dissolved Oxygen, AA - Abundance of autotrophs, AB - Biomass of autotrophs, AV - Biovolume of autotrophs, HA - Abundance of heterotrophs, HB - Biomass of heterotrophs, HV - Biovolume of heterotrophs, NEM - Northeast Monsoon, PSWM - Pre-Southwest Monsoon, SWM - Southwest Monsoon.

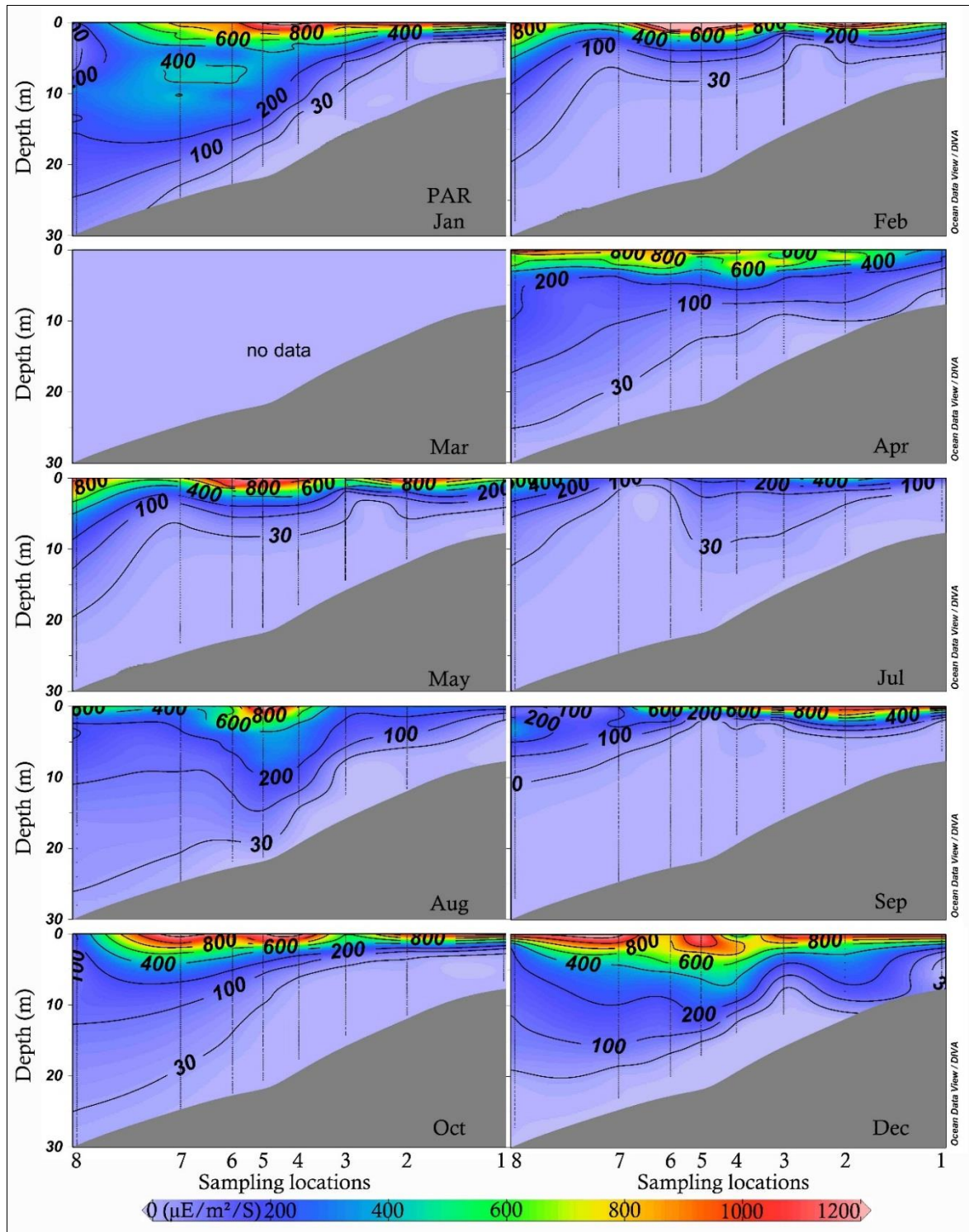


Sur.	JAN	FEB	MAR	APR	MAY	JUL	AUG	SEP	OCT	DEC
TEM	28.95 (0.12)	30.12 (0.17)	30.44 (0.18)	31.32 (0.09)	30.09 (0.14)	27.12 (0.13)	28.03 (0.02)	27.23 (0.36)	29.36 (0.19)	30 (0.32)
SAL	33.33 (0.78)	33.97 (0.17)	32.99 (1.16)	34.01 (0.18)	33.95 (0.1)	19.92 (4.09)	31.26 (0.76)	35.18 (0.12)	28.62 (1.43)	32.21 (0.77)
PAR	728 (222)	710 (247)	NA	396 (132)	702 (253)	95 (36)	398 (222)	286 (62)	851 (196)	1036 (179)
TUR	2.37 (1.67)	2.32 (0.34)	NA	0.68 (0.35)	2.32 (0.34)	4.58 (3.23)	4.06 (1.09)	3.56 (1.9)	4.01 (1.54)	2.13 (1.13)
NO <sub>3</sub>	1.11 (0.47)	0.18 (0.04)	0.9 (0.12)	0.45 (0.14)	1.11 (0.7)	1.05 (0.3)	1.18 (0.2)	1.82 (0.74)	3.47 (0.48)	1.45 (0.35)
PO <sub>4</sub>	0.74 (0.21)	0.46 (0.06)	0.42 (0.13)	0.83 (0.28)	0.53 (0.09)	1.19 (0.32)	1.11 (0.37)	3.07 (0.41)	1.1 (0.25)	0.18 (0.04)
SiO <sub>4</sub>	3.8 (0.8)	13.02 (2.96)	10.91 (1.38)	4.63 (0.76)	6.39 (2.12)	30.85 (7.84)	16.85 (10.27)	24.78 (2.05)	21.87 (7.05)	20.08 (3.58)
DO	7.2 (0.39)	6.27 (0.16)	5.99 (0.64)	3.78 (0.75)	3.59 (0.67)	8.29 (0.49)	4.72 (1.02)	8.41 (1.63)	6.69 (0.16)	9.5 (0.83)
CHL	1.21 (0.73)	0.92 (0.28)	1.54 (0.94)	0.29 (0.26)	0.92 (0.28)	2.88 (0.54)	0.47 (0.02)	14.65 (7.67)	0.83 (0.06)	1 (0.88)
AA	1323 (689)	2700 (1607)	22497 (16913)	5263 (1837)	20831 (16126)	10510 (1630)	5173 (3035)	12443 (3415)	3474 (955)	18871 (4984)
AB	2.03 (1.01)	4.51 (1.99)	18.36 (10.39)	10.94 (5.91)	20.57 (10.51)	15.06 (6.59)	6.73 (2.09)	19.48 (6.12)	7.47 (3.16)	18.06 (6.15)
AV	87160 (43930)	61815 (10606)	46240 (14751)	38477 (8756)	30707 (7373)	32979 (8004)	64638 (17128)	65975 (30556)	62277 (10902)	24744 (1576)
HA	146 (103)	715 (527)	658 (528)	809 (386)	1152 (863)	1430 (483)	266 (47)	703 (181)	890 (503)	291 (204)
HB	2.8 (2.07)	5.74 (3.29)	11.61 (9.27)	5.88 (2.99)	10.8 (6.52)	19 (3.35)	5.08 (0.6)	5.32 (1.84)	14.89 (9.26)	2.31 (1.16)
HV	301503 (53383)	152223 (32878)	288427 (63885)	96448 (16537)	211994 (56395)	191872 (31685)	250565 (38341)	82369 (15575)	186534 (35049)	146272 (35184)
Mid.	JAN	FEB	MAR	APR	MAY	JUL	AUG	SEP	OCT	DEC
TEM	28.4 (0.1)	29.05 (0.08)	29.82 (0.09)	30.12 (0.29)	29.04 (0.08)	25.82 (0.54)	27.75 (0.02)	25.76 (0.48)	28.77 (0.03)	29.04 (0.05)
SAL	34.29 (0.21)	34.35 (0.09)	34.08 (0.03)	34.26 (0.11)	34.35 (0.09)	33.63 (0.82)	34.86 (0.3)	35.27 (0.07)	34.47 (0.27)	33.23 (0.19)
PAR	243 (72)	17 (6)	NA	91 (27)	17 (6)	24 (12)	117 (37)	4 (2)	34 (18)	157 (43)
TUR	0.74 (0.37)	1.52 (0.32)	NA	0.5 (0.1)	1.52 (0.32)	0.4 (0.02)	0.44 (0)	0.86 (0.28)	1.9 (1.33)	1.12 (0.66)
NO <sub>3</sub>	0.62 (0.1)	0.23 (0.07)	0.88 (0.22)	0.56 (0.11)	0.54 (0.17)	7.53 (1.13)	3.18 (0.67)	8.55 (2.66)	2.04 (0.51)	1.22 (0.11)
PO <sub>4</sub>	0.15 (0.01)	0.33 (0.03)	0.29 (0.15)	0.86 (0.33)	0.13 (0.13)	1.35 (0.34)	0.84 (0.16)	2.68 (0.45)	0.58 (0.17)	0.25 (0.13)
SiO <sub>4</sub>	2.19 (0.82)	8.42 (0.95)	10.21 (3.07)	3.52 (1.31)	4.42 (1.3)	11.7 (1.79)	9.58 (0.56)	15.3 (4.81)	6.99 (2.23)	12.56 (0.45)
DO	6.31 (0.05)	6.16 (0.51)	6.46 (0.16)	3.69 (0.92)	4.15 (0.24)	5.14 (0.92)	5.59 (0.56)	3.24 (1.93)	5.89 (0.55)	8.27 (0.53)
CHL	0.4 (0.35)	0.45 (0.15)	0.2 (0.07)	0.58 (0.25)	0.45 (0.15)	1.6 (0.14)	0.2 (0.02)	2.56 (1.46)	0.56 (0.05)	0.17 (0)

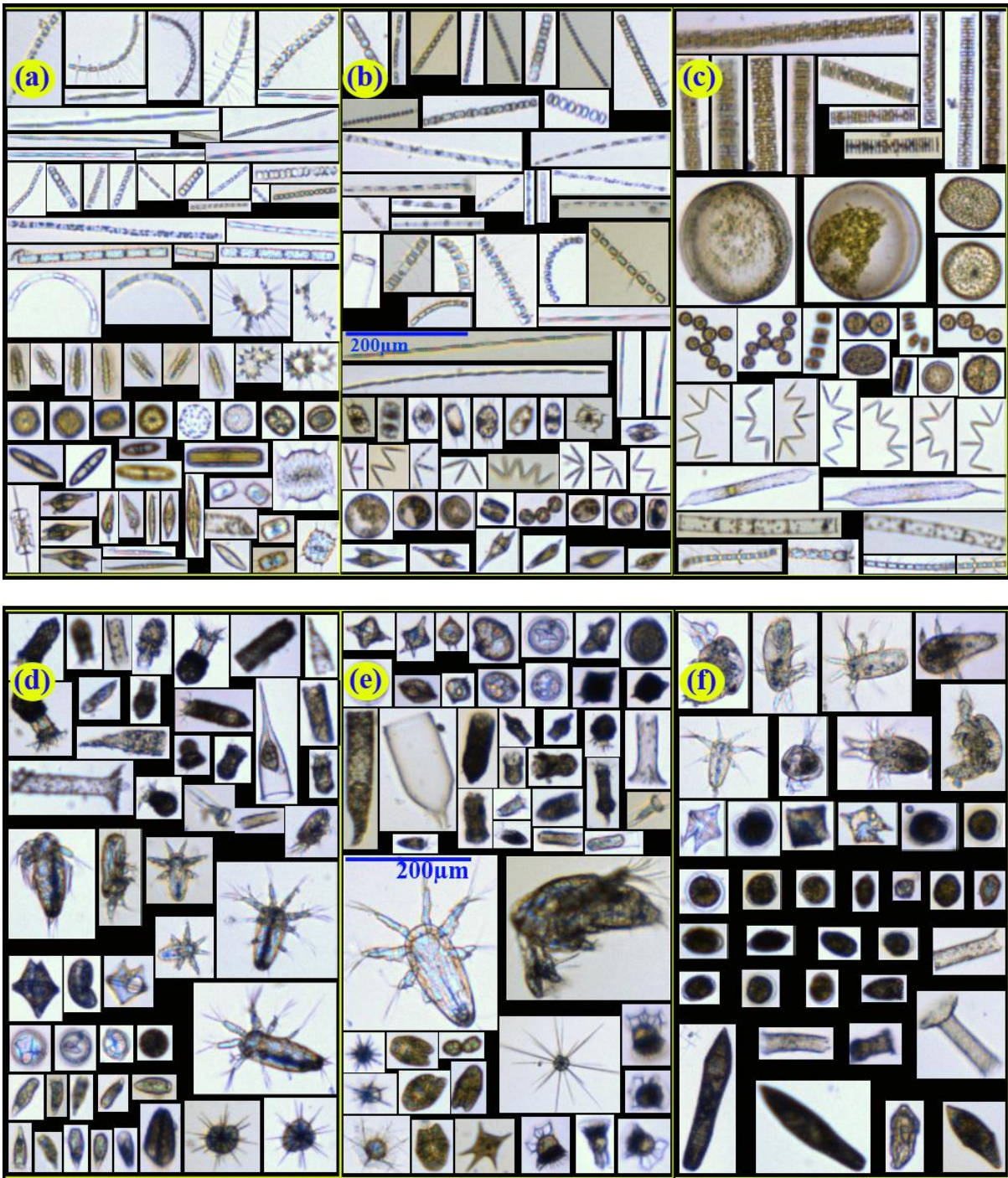
AA	1960 (1386)	352 (111)	2351 (1342)	1296 (43)	8055 (2696)	4370 (2565)	772 (592)	6728 (4368)	1082 (192)	6287 (3366)
AB	2.79 (1.46)	0.73 (0.24)	5.31 (2.82)	4.14 (0.18)	7.75 (2)	12.51 (9.62)	1.3 (0.56)	13.18 (5.43)	5.51 (2.97)	8.22 (4.09)
AV	67177 (20052)	59321 (7115)	50362 (3605)	77607 (3788)	24308 (5318)	74822 (28448)	79008 (20741)	106616 (41523)	252775 (197959)	41674 (3888)
HA	156 (61)	305 (61)	213 (32)	487 (107)	343 (66)	478 (123)	245 (67)	438 (183)	518 (129)	237 (120)
HB	4.28 (1.12)	3.89 (0.91)	3.62 (0.43)	6.82 (0.63)	4.43 (0.49)	9.15 (1.52)	5.09 (1.57)	6.61 (2.24)	6.78 (0.33)	4.11 (2.39)
HV	395321 (48787)	172272 (7242)	271044 (18083)	219207 (66745)	194584 (31643)	286788 (107967)	260986 (16219)	279855 (62925)	199789 (65428)	205464 (13656)
<b>Bot.</b>	JAN	FEB	MAR	APR	MAY	JUL	AUG	SEP	OCT	DEC
TEM	28.5 (0.16)	29.15 (0.16)	29.68 (0.21)	29.89 (0.4)	29.21 (0.22)	24.33 (0.74)	26.97 (0.51)	24.41 (0.5)	28.33 (0.13)	29.29 (0.37)
SAL	33.64 (1.06)	34.67 (0.19)	34.13 (0.01)	34.27 (0.11)	34.63 (0.23)	31.63 (2.91)	33.54 (1.88)	35.41 (0.06)	35.22 (0.27)	33.37 (0.57)
PAR	1.7 (0.7)	2.4 (2.1)	NA	11.8 (11.3)	2.3 (1.9)	0.2 (0.2)	13.1 (7.7)	0.1 (0)	1.2 (1.1)	0.7 (0.3)
TUR	8.82 (1.76)	8.15 (2)	NA	5.32 (1.86)	8.15 (2)	12.36 (2.01)	7.94 (2.25)	7.14 (1.87)	5.88 (2.61)	17.05 (2.76)
NO <sub>3</sub>	0.67 (0.28)	1.13 (0.52)	1.1 (0.28)	0.87 (0.05)	1.54 (0.65)	15.52 (3.81)	6.03 (2.49)	14.23 (0.91)	1.86 (0.36)	1.41 (0.2)
PO <sub>4</sub>	0.54 (0.17)	0.35 (0.11)	0.4 (0.11)	1.2 (0.18)	0.31 (0.1)	1.73 (0.12)	0.83 (0.12)	3.17 (0.32)	0.85 (0.15)	0.4 (0.07)
SiO <sub>4</sub>	3.24 (0.29)	8.48 (0.68)	9.82 (1.72)	6.24 (1.16)	10.96 (1.78)	22.86 (2.09)	9.92 (0.72)	19.15 (3.64)	7.72 (0.92)	17.72 (2.26)
DO	6.23 (0.14)	5.35 (0.16)	5.64 (0.46)	3.34 (0.38)	2.29 (0.29)	1.36 (0.62)	5.27 (0.78)	3.7 (2.53)	5.33 (0.37)	6.67 (0.27)
CHL	0.92 (0.26)	0.39 (0.08)	0.9 (0.32)	0.38 (0.05)	0.39 (0.08)	1.9 (0.45)	0.29 (0.11)	0.96 (0.66)	0.27 (0.08)	0.92 (0.16)
AA	2394 (851)	1234 (336)	7200 (5675)	2150 (727)	2826 (859)	17105 (4005)	3144 (2154)	6275 (3625)	765 (442)	12900 (6121)
AB	4.8 (0.94)	2.75 (0.56)	10.28 (3.91)	6.79 (1.65)	5.38 (1.77)	54.53 (13.7)	3.94 (2.08)	18.69 (10.26)	1.47 (0.75)	14.74 (4.81)
AV	88852 (19954)	66347 (9038)	122152 (36366)	83678 (6762)	57899 (7324)	100509 (14096)	54135 (9706)	122731 (5992)	71361 (16671)	46220 (6929)
HA	175 (72)	259 (81)	533 (296)	795 (515)	800 (449)	1148 (790)	136 (24)	209 (105)	225 (111)	705 (307)
HB	3.08 (1.05)	2.81 (1.07)	8.32 (4.18)	9.75 (6.06)	8.41 (4.07)	6.1 (3.07)	2.25 (0.68)	4.93 (3.02)	2.35 (0.84)	7.23 (3.21)
HV	271274 (52453)	165374 (27919)	239652 (47686)	175616 (29794)	164302 (5546)	117740 (29816)	226735 (30908)	228620 (108043)	168773 (37653)	143490 (6396)

**Table 2** - Physicochemical and biological parameters at different depths presented. Abbreviations: TEM - temperature (°C); SAL - salinity (PSU); PAR - photosynthetically available radiation ( $\mu\text{E}/\text{m}^2/\text{day}$ ); TUR - turbidity (NTU); NO<sub>3</sub> - nitrate ( $\mu\text{M}/\text{L}$ ); PO<sub>4</sub> - phosphate ( $\mu\text{M}/\text{L}$ ); SiO<sub>4</sub> - silicate ( $\mu\text{M}/\text{L}$ ); DO - dissolved oxygen (ml/L); CHL - chlorophyll-a ( $\mu\text{g}/\text{L}$ ); AA - abundance of autotrophs (individual/L); AB - biomass of autotrophs ( $\mu\text{g C}/\text{L}$ ); AV - biovolume of autotrophs ( $\mu\text{m}^3/\text{individual}$ ); HA - abundance of heterotrophs (individual/L); HB - biomass of heterotrophs ( $\mu\text{g C}/\text{L}$ ) and HV - biovolume of heterotrophs ( $\mu\text{m}^3/\text{individual}$ ). SE in parenthesis.

Supplementary Materials



**Supplementary Figure 1** - Monthly vertical distribution of Photosynthetically Active Radiation (PAR) along the study transect off Kochi. No data presented for June and November.



**Supplementary Figure 2** - FlowCAM images of micro-autotrophs found during (a) NEM, (b) PSWM and (c) SWM and the micro-heterotrophs found during (d) NEM, (e) PSWM and (f) SWM.

**Supplementary Table 1** - The seasonal distribution of physico-chemical and biological parameters in coastal to offshore water and in the vertical water column. Table presented the mean and standard error in parenthesis. Abbreviations: TEM - Temperature, SAL - Salinity, PAR - Photosynthetically available radiation, TUR - Turbidity, NO<sub>3</sub> - Nitrate, PO<sub>4</sub> - Phosphate, SiO<sub>4</sub> - Silicate, DO - Dissolved Oxygen, AA - Abundance of autotrophs, AB - Biomass of autotrophs, AV - Biovolume of autotrophs, HA - Abundance of heterotrophs, HB - Biomass of heterotrophs, HV - Biovolume of heterotrophs, NEM - North East Monsoon, PSWM - Pre-Southwest Monsoon, SWM - Southwest Monsoon, S - Surface, M - Middle, B - Bottom, 1-7 - Sampling locations from coastal to offshore.

	TEM (°C)	SAL (PSU)	PAR ( $\mu\text{E}/\text{m}^2$ )	TUR (NTU)	NO <sub>3</sub> ( $\mu\text{M}/\text{L}$ )	PO <sub>4</sub> ( $\mu\text{M}/\text{L}$ )	SiO <sub>4</sub> ( $\mu\text{M}/\text{L}$ )	DO (ml/L)	CHL ( $\mu\text{g}/\text{L}$ )	AA (Ind./L)	AB ( $\mu\text{gC}/\text{L}$ )	AV ( $\mu\text{m}^3/\text{ind.}$ )	HA (Ind./L)	HB ( $\mu\text{gC}/\text{L}$ )	HV ( $\mu\text{m}^3/\text{ind.}$ )
NEM-S	29.7 (0.2)	33.2 (0.4)	824.5 (122.5)	2.27 (0.62)	0.84 (0.28)	0.43 (0.12)	11.77 (3.37)	7.06 (0.9)	1.03 (0.32)	8003 (2217)	8.08 (2.2)	49705 (12209)	450 (170)	4.13 (1.17)	186843 (24064)
NEM-M	28.8 (0.11)	34 (0.2)	139.1 (40.9)	1.13 (0.26)	0.93 (0.32)	0.36 (0.12)	8.46 (2.25)	6.1 (0.94)	0.34 (0.12)	2536 (1030)	3.56 (1.26)	51968 (5799)	332 (75)	4.93 (0.91)	231998 (31368)
NEM-B	28.9 (0.17)	33.9 (0.4)	1.6 (0.7)	11.34 (1.68)	1.09 (0.15)	0.49 (0.07)	11.37 (3.38)	5.34 (0.79)	0.74 (0.12)	4697 (1851)	6.38 (1.68)	62025 (7026)	379 (91)	4.22 (0.92)	185007 (18825)
PSWM-S	30.6 (0.17)	33.6 (0.38)	549.3 (144.2)	1.5 (0.38)	0.82 (0.19)	0.59 (0.12)	7.31 (1.87)	4.45 (0.77)	0.97 (0.36)	16197 (7445)	16.6 (4.96)	38475 (5945)	873 (332)	9.43 (3.62)	198956 (35372)
PSWM-M	29.7 (0.18)	34.2 (0.06)	54.1 (20.7)	1.01 (0.27)	0.66 (0.11)	0.42 (0.22)	6.05 (2.1)	4.77 (0.86)	0.41 (0.1)	3901 (1163)	5.74 (1.13)	50759 (7989)	348 (54)	4.96 (0.55)	228278 (24675)
PSWM-B	29.5 (0.18)	34.3 (0.1)	7 (5.6)	6.73 (1.37)	1.17 (0.2)	0.64 (0.28)	9.01 (1.42)	3.75 (0.99)	0.56 (0.12)	4059 (1870)	7.48 (1.52)	87910 (13879)	709 (228)	8.83 (2.54)	193190 (19756)
SWM-S	27.4 (0.17)	28.6 (2.52)	259.9 (79.7)	4.07 (1.27)	1.35 (0.24)	1.79 (0.64)	24.16 (4.05)	7.14 (1.21)	8.12 (3.76)	7900 (1459)	12.2 (2.58)	56468 (9104)	822 (194)	11.1 (2.73)	177835 (21020)
SWM-M	26.3 (0.4)	34.5 (0.39)	48.4 (20.7)	0.58 (0.12)	6.42 (1.65)	1.62 (0.55)	12.19 (1.67)	4.66 (0.72)	1.61 (0.59)	3238 (1317)	8.12 (2.86)	128305 (48980)	420 (65)	6.91 (0.8)	256855 (31987)
SWM-B	25.1 (0.48)	33.5 (1.17)	4.5 (3)	9.26 (1.29)	11.93 (2.97)	1.91 (0.68)	17.31 (3.85)	3.44 (1.14)	1.33 (0.34)	6822 (2075)	19.7 (6.7)	137184 (10196)	429 (210)	3.91 (1.08)	185467 (29787)
NEM-1	29.9 (0.31)	31.8 (0.68)	224.4 (107.7)	7.43 (1.34)	0.77 (0.37)	0.31 (0.02)	10.61 (2.81)	6.37 (0.87)	1.77 (0.34)	11268 (4023)	13 (4.1)	40492 (4135)	1068 (262)	9.4 (1.6)	157897 (27152)
NEM-3	29.1 (0.19)	34.1 (0.15)	258.1 (113.5)	5.42 (2.2)	0.94 (0.35)	0.42 (0.08)	11.7 (3.48)	5.77 (0.88)	0.69 (0.12)	4525 (1452)	5.3 (1.4)	44700 (5011)	339 (76)	4.6 (0.9)	194493 (15284)
NEM-5	29 (0.17)	33.9 (0.26)	520.2 (218.3)	4.93 (2.52)	0.85 (0.18)	0.46 (0.1)	8.61 (2.7)	6 (0.6)	0.36 (0.11)	4804 (2162)	5.6 (1.7)	59361 (8813)	224 (52)	3 (0.7)	212259 (32943)
NEM-7	29 (0.19)	34.2 (0.26)	312.7 (144.7)	3.96 (1.77)	1.42 (0.2)	0.59 (0.16)	12.59 (3.61)	6.75 (1.17)	0.36 (0.08)	2628 (1149)	3.2 (1)	69885 (15821)	162 (35)	2.2 (0.5)	215781 (32316)
PSWM-1	30.6 (0.25)	33.1 (0.73)	119.6 (56.1)	4.48 (2.57)	0.99 (0.18)	0.47 (0.1)	7.59 (2.4)	4.73 (0.69)	1.62 (0.59)	19607 (10974)	23 (5.8)	45601 (8437)	2303 (313)	25.4 (3.5)	155065 (23113)
PSWM-3	29.9 (0.24)	34.2 (0.07)	178 (112.3)	2.55 (0.9)	0.84 (0.12)	0.7 (0.43)	6.38 (1.07)	3.95 (0.95)	0.42 (0.09)	12441 (7281)	13.8 (4.8)	59738 (15581)	402 (50)	5.3 (0.8)	186885 (23313)
PSWM-5	29.9 (0.25)	34.2 (0.08)	332.2 (229.8)	3.09 (1.47)	0.66 (0.15)	0.43 (0.14)	7.31 (1.1)	4.49 (1.33)	0.48 (0.13)	1780 (313)	3.8 (0.3)	68541 (16619)	241 (25)	3.9 (0.6)	252684 (37143)
PSWM-7	29.7 (0.25)	34.4 (0.1)	206 (121.9)	3.37 (1.73)	1.25 (0.49)	0.79 (0.22)	9.78 (2.74)	3.8 (0.88)	0.41 (0.06)	3616 (1248)	4.9 (0.7)	60591 (11154)	278 (58)	3.1 (0.4)	208195 (32175)
SWM-1	26.9 (0.39)	27 (4.18)	80.1 (53.6)	10.27 (1.91)	6.95 (1.11)	1.62 (0.4)	12.82 (2.04)	4.18 (0.37)	2.62 (0.24)	14017 (1644)	36 (10.4)	75769 (20358)	1317 (596)	9.1 (3.7)	137857 (41784)
SWM-3	25.9 (0.55)	32.3 (2.14)	106.3 (49)	3.84 (1.6)	6.47 (0.74)	1.59 (0.62)	14.52 (3.2)	5.34 (0.57)	7.15 (4.74)	6144 (1697)	14.9 (5.3)	83793 (18490)	491 (129)	6.4 (1.5)	185100 (23719)
SWM-5	26.2 (0.58)	33.8 (0.84)	183.4 (112.8)	3.8 (1.63)	7.71 (3.02)	1.94 (0.88)	19.6 (5.09)	4.86 (0.47)	4.3 (2.96)	8388 (3358)	14.2 (7.4)	96031 (12434)	347 (73)	6.4 (1.6)	206993 (41374)
SWM-7	26.1 (0.61)	33.3 (1.5)	57.9 (27.6)	3.6 (1.41)	4.49 (1.79)	2.12 (0.58)	30.83 (3.5)	6.58 (0.85)	0.96 (0.47)	4368 (1443)	8.6 (3.4)	97716 (12603)	402 (131)	7.1 (2.4)	279834 (44552)

**Supplementary Table 2 – Composition and abundance of microplankton during different seasons**

Sl. No	Autotrophs	NEM-1	NEM-3	NEM-5	NEM-7	PSWM-1	PSWM-3	PSWM-5	PSWM-7	SWM-1	SWM-3	SWM-5	SWM-7
1	<i>Amphiprora</i>	43±16	51±18	21±9	97±57	96±54	32±16	7±2	53±34	20±12	33±28	20±15	---
2	<i>Asterionella</i>	523±76	105±32	65±15	95±60	312±188	143±75	4±1	36±32	270±78	139±59	563±405	358±226
3	<i>Cerataulina</i>	99±17	44±12	53±22	38±13	555±462	166±77	66±14	105±31	75±17	93±9	123±48	26±7
4	<i>Ceratium</i>	818±691	59±27	28±5	22±7	1862±1167	68±21	38±7	66±11	180±131	57±24	54±26	26±7
5	<i>Chaetoceros</i>	1745±873	1224±530	1419±839	549±317	805±479	1170±601	266±103	614±378	850±431	540±204	1437±875	528±241
6	<i>Corethron</i>	24±10	22±7	21±11	10±5	38±10	49±26	10±2	41±19	---	5±3	5±2	5±3
7	<i>Coscinodiscus</i>	10±6	7±3	8±2	40±30	10±3	11±5	5±2	3±1	120±42	51±15	13±7	25±9
8	<i>Cyclotella</i>	8±4	2±1	---	---	---	---	---	---	---	---	5±4	---
9	<i>Dactyliosolen</i>	261±116	180±53	142±79	194±149	300±88	17±4	15±5	18±4	---	---	140±98	33±8
10	<i>Ditylum</i>	131±50	59±15	46±15	29±17	78±25	59±36	19±6	135±116	20±12	---	20±15	---
11	<i>Eucampia</i>	26±8	7±3	13±4	8±3	80±36	16±6	8±3	30±25	20±10	90±65	160±88	63±23
12	<i>Fragilaria</i>	172±66	84±40	166±86	109±36	37±3	53±18	93±50	199±90	1350±715	1228±626	1113±953	476±237
13	<i>Gomphonema</i>	---	---	---	---	---	35±15	21±6	43±10	---	---	---	---
14	<i>Guinardia</i>	53±26	68±19	33±7	30±13	193±113	118±29	48±15	141±55	150±47	231±183	671±425	180±100
15	<i>Haslea</i>	20±7	7±3	4±3	---	40±16	14±4	8±3	10±3	---	---	---	10±6
16	<i>Hemiaulus</i>	20±6	9±2	11±4	14±7	40±24	25±7	20±5	35±23	---	9±6	13±8	---
17	<i>Lauderia</i>	19±5	8±6	6±2	7±3	60±26	11±5	4±2	55±49	---	---	45±15	---
18	<i>Leptocylindrus</i>	741±386	478±130	654±266	406±274	1083±791	870±214	263±69	1552±764	493±159	192±41	256±79	184±60
19	<i>Melosira</i>	16±10	45±38	9±4	6±2	---	3±1	2±1	2±1	30±10	55±0	35±5	24±6
20	<i>Meuniera</i>	20±12	5±2	7±4	7±3	43±17	14±6	6±1	11±2	---	---	---	---
21	<i>Navicula</i>	10±7	43±27	25±13	20±8	37±22	21±8	8±3	32±11	---	---	---	8±3
22	<i>Nitzschia</i>	124±49	111±59	72±44	124±67	274±163	61±16	36±15	76±30	364±191	63±29	79±49	42±23
23	<i>Odontella</i>	185±52	66±26	47±15	42±20	550±271	514±448	63±36	60±19	1132±366	249±81	573±508	182±160
24	<i>Paralia</i>	19±8	27±9	15±3	10±5	27±7	15±13	8±3	11±5	---	---	---	---
25	<i>Planktoniella</i>	10±5	6±2	3±1	2±1	---	8±3	15±5	13±5	---	5±2	---	55±48
26	<i>Pleurosigna</i>	101±39	143±83	27±11	42±16	180±140	34±8	6±1	51±23	400±272	51±26	82±40	33±16
27	<i>Pseudo-nitzschia</i>	2088±1413	1415±706	1496±1091	445±242	1060±140	734±424	112±42	189±75	1533±679	198±47	236±92	77±21
28	<i>Rhizosolenia</i>	81±27	54±18	59±17	36±10	248±143	130±19	63±8	95±18	287±85	241±68	322±129	223±70
29	<i>Skeletonema</i>	3964±1620	392±111	419±172	320±151	12005±11259	6908±6316	125±23	389±223	967±495	537±349	1188±956	371±249
30	<i>Streptotheca</i>	73±56	45±26	27±10	11±7	82±35	38±8	6±2	82±59	20±14	5±3	---	---
31	<i>Surirella</i>	44±36	1±1	20±13	22±9	40±17	30±10	6±4	25±5	---	75±48	120±85	---
32	<i>Thalassionema</i>	156±49	50±18	33±6	36±16	296±192	101±46	62±26	221±155	1043±626	702±520	701±548	1104±1002
33	<i>Thalassiosira</i>	230±74	120±39	84±34	51±23	297±67	95±37	72±25	188±72	3793±1401	1442±716	1524±927	976±585
34	<i>Cyanobacteria</i>	---	6±4	20±13	7±2	28±5	124±40	93±14	101±16	---	---	18±10	10±4
35	<i>Dinophysis</i>	43±14	25±22	7±4	2±1	132±58	15±3	10±2	13±3	1000±910	55±22	28±8	11±2
36	<i>Oxytoxum</i>	---	---	2±1	2±1	---	---	3±1	8±5	---	---	---	---
37	<i>Polysphaeridium</i>	---	7±4	1±1	3±1	---	22±19	3±1	8±2	---	---	5±3	15±7
38	<i>Prorocentrum</i>	57±33	36±14	13±5	7±2	68±25	9±3	4±1	15±4	20±13	20±11	13±8	5±3
39	<i>Dictyocha</i>	12±8	35±5	45±32	---	65±22	7±3	8±2	12±8	20±13	20±12	13±8	10±5
40	Unidentified	453±106	266±60	328±93	439±247	1188±942	1395±777	435±198	532±214	707±317	423±69	431±150	268±80
	<b>Heterotrophs</b>	<b>NEM-1</b>	<b>NEM-3</b>	<b>NEM-5</b>	<b>NEM-7</b>	<b>PSWM-1</b>	<b>PSWM-3</b>	<b>PSWM-5</b>	<b>PSWM-7</b>	<b>SWM-1</b>	<b>SWM-3</b>	<b>SWM-5</b>	<b>SWM-7</b>
41	<i>Gymnodinium</i>	326±297	17±12	23±17	---	510±272	128±82	18±8	158±96	---	140±65	40±20	100±95
42	<i>Gyrodinium</i>	5±2	3±1	7±2	8±3	30±15	6±1	7±2	15±6	20±7	---	45±15	10±5
43	<i>Noctiluca</i>	4±3	2±1	2±1	2±1	20±6	3±1	2±1	5±2	---	---	---	---
44	<i>Ornithocercus</i>	---	11±9	18±3	---	90±38	61±59	18±16	121±109	20±8	7±2	20±15	40±16
45	<i>Podolampus</i>	---	5±3	8±5	---	10±4	5±2	---	10±4	---	---	40±26	10±4
46	<i>Polykrikos</i>	10±5	5±3	---	---	20±9	---	---	2±1	---	60±29	40±20	10±5
47	<i>Protoperidinium</i>	220±56	80±25	35±9	26±8	908±302	121±36	64±9	165±87	473±199	238±116	79±21	96±32
48	<i>Stelladinium</i>	---	8±5	13±7	---	---	---	---	15±5	---	15±6	20±24	---
49	<i>Favella</i>	10±4	---	6±4	---	30±29	---	---	---	40±31	5±3	---	---
50	<i>Mesodinium</i>	---	1±1	---	6±3	---	2±1	---	---	---	8±3	30±18	20±12
51	<i>Strombidium</i>	180±112	---	10±6	10±6	40±25	---	---	---	40±20	---	---	---
52	<i>Tintinnopsis</i>	423±119	113±30	89±31	51±15	625±137	95±25	58±19	81±27	900±739	48±21	41±21	50±31
53	<i>Nauplius</i>	177±86	118±34	73±16	63±17	342±63	105±20	78±13	88±16	365±217	242±99	208±66	221±108
54	<i>Foraminifera</i>	35±23	34±17	4±1	7±3	30±10	9±3	10±4	29±19	20±15	14±10	20±13	8±3
55	<i>Acanthometron</i>	47±13	19±4	10±2	14±6	160±100	29±6	21±3	22±5	---	5±3	10±5	43±28
56	<i>Radiolaria</i>	6±4	7±5	11±5	22±13	---	---	---	12±4	---	---	5±3	---
57	Unidentified	59±16	12±3	10±2	21±6	50±13	59±38	7±1	18±6	30±10	33±16	19±3	25±14

**Supplementary Table 3 - Composition and size ( $\pm$  SE) of microplankton during different seasons**

Autotrophs	NEM-1	NEM-3	NEM-5	NEM-7	PSWM-1	PSWM-3	PSWM-5	PSWM-7	SWM-1	SWM-3	SWM-5	SWM-7
<i>Amphiprora</i>	34277 $\pm$ 1030	38066 $\pm$ 920	33647 $\pm$ 2930	42683 $\pm$ 1657	45327 $\pm$ 1153	56508 $\pm$ 4647	54200 $\pm$ 2637	50805 $\pm$ 2284	17700 $\pm$ 1245	34431 $\pm$ 2021	31000 $\pm$ 1854	---
<i>Asterionella</i>	43585 $\pm$ 910	38527 $\pm$ 1981	29323 $\pm$ 1155	28675 $\pm$ 1261	37312 $\pm$ 1296	32400 $\pm$ 1183	46700 $\pm$ 11778	57635 $\pm$ 4201	22865 $\pm$ 530	27446 $\pm$ 1016	18532 $\pm$ 281	20534 $\pm$ 518
<i>Cerataulima</i>	55518 $\pm$ 2956	48041 $\pm$ 2996	48082 $\pm$ 2225	66345 $\pm$ 6471	34470 $\pm$ 700	37417 $\pm$ 1165	30341 $\pm$ 1383	34180 $\pm$ 958	37893 $\pm$ 1721	24888 $\pm$ 772	36160 $\pm$ 1779	29744 $\pm$ 1390
<i>Chaetoceros</i>	37450 $\pm$ 383	35330 $\pm$ 440	39522 $\pm$ 616	43927 $\pm$ 1013	36783 $\pm$ 833	25956 $\pm$ 400	39329 $\pm$ 2187	47279 $\pm$ 905	53925 $\pm$ 2461	37991 $\pm$ 988	25208 $\pm$ 316	30170 $\pm$ 892
<i>Corethron</i>	33730 $\pm$ 1149	32029 $\pm$ 1555	27500 $\pm$ 1736	39500 $\pm$ 1866	32013 $\pm$ 627	25190 $\pm$ 664	23684 $\pm$ 1395	35540 $\pm$ 1415	---	22000 $\pm$ 1150	42500 $\pm$ 2410	27200 $\pm$ 1352
<i>Coscinodiscus</i>	191000 $\pm$ 97544	1322794 $\pm$ 85425	2090600 $\pm$ 270933	342833 $\pm$ 65281	184400 $\pm$ 15857	964647 $\pm$ 154896	1458100 $\pm$ 219904	1162633 $\pm$ 352510	4020778 $\pm$ 222296	1911623 $\pm$ 62332	2184333 $\pm$ 219087	1479233 $\pm$ 95883
<i>Dactyliosolen</i>	28539 $\pm$ 566	18026 $\pm$ 403	22432 $\pm$ 872	28682 $\pm$ 739	17511 $\pm$ 844	60523 $\pm$ 7739	43003 $\pm$ 12752	52172 $\pm$ 2952	---	---	13356 $\pm$ 651	19095 $\pm$ 1317
<i>Ditylum</i>	124114 $\pm$ 2263	138560 $\pm$ 4707	135675 $\pm$ 4218	122882 $\pm$ 5368	145164 $\pm$ 3746	120243 $\pm$ 3718	103467 $\pm$ 5495	165137 $\pm$ 3889	41400 $\pm$ 5655	---	39700 $\pm$ 5402	---
<i>Eucampia</i>	63899 $\pm$ 6683	41454 $\pm$ 7210	65515 $\pm$ 5210	32933 $\pm$ 6627	19150 $\pm$ 242	79840 $\pm$ 10425	91513 $\pm$ 22118	33920 $\pm$ 4997	9830 $\pm$ 584	29733 $\pm$ 1420	20382 $\pm$ 764	19869 $\pm$ 2094
<i>Fragilaria</i>	82404 $\pm$ 3818	110327 $\pm$ 7775	215966 $\pm$ 9950	96872 $\pm$ 6206	67491 $\pm$ 5161	100219 $\pm$ 12247	59756 $\pm$ 3690	65151 $\pm$ 2319	191393 $\pm$ 3514	210792 $\pm$ 3294	204523 $\pm$ 3790	237665 $\pm$ 6049
<i>Gomphonema</i>	---	---	---	---	---	68979 $\pm$ 16422	42610 $\pm$ 3597	26878 $\pm$ 1164	---	---	---	---
<i>Guinardia</i>	134472 $\pm$ 9649	119305 $\pm$ 11081	109619 $\pm$ 6986	78539 $\pm$ 7925	110578 $\pm$ 4053	48256 $\pm$ 1162	45442 $\pm$ 2535	83995 $\pm$ 2507	53615 $\pm$ 1533	48091 $\pm$ 1271	40238 $\pm$ 919	44189 $\pm$ 2319
<i>Haslea</i>	144150 $\pm$ 14972	191338 $\pm$ 20439	70986 $\pm$ 4864	---	77750 $\pm$ 5484	149933 $\pm$ 7138	186024 $\pm$ 24737	136900 $\pm$ 11251	---	---	---	22250 $\pm$ 1317
<i>Hemiaulus</i>	116817 $\pm$ 14074	139163 $\pm$ 15139	109308 $\pm$ 11179	107122 $\pm$ 10053	70138 $\pm$ 4874	84322 $\pm$ 9817	72730 $\pm$ 6583	50380 $\pm$ 2448	---	61600 $\pm$ 4246	47200 $\pm$ 3021	---
<i>Lauderia</i>	105362 $\pm$ 11395	75273 $\pm$ 18889	170478 $\pm$ 26022	131007 $\pm$ 14569	93033 $\pm$ 3335	46425 $\pm$ 2184	24700 $\pm$ 1438	51374 $\pm$ 1513	---	---	50656 $\pm$ 3381	---
<i>Leptocylindrus</i>	24301 $\pm$ 430	18383 $\pm$ 327	20033 $\pm$ 445	18212 $\pm$ 581	15166 $\pm$ 219	15274 $\pm$ 283	13875 $\pm$ 533	10206 $\pm$ 123	14746 $\pm$ 307	15110 $\pm$ 560	15866 $\pm$ 488	14561 $\pm$ 407
<i>Melosira</i>	331950 $\pm$ 81253	160933 $\pm$ 7096	54082 $\pm$ 7683	86022 $\pm$ 16041	---	70533 $\pm$ 2509	133000 $\pm$ 17548	39600 $\pm$ 3548	119900 $\pm$ 14852	135427 $\pm$ 12091	134671 $\pm$ 10329	411723 $\pm$ 72256
<i>Menniera</i>	11430 $\pm$ 911	75608 $\pm$ 15055	89075 $\pm$ 12548	87193 $\pm$ 15249	84725 $\pm$ 5107	73004 $\pm$ 7994	40217 $\pm$ 4662	141451 $\pm$ 16019	---	---	---	---
<i>Navicula</i>	69800 $\pm$ 2658	89801 $\pm$ 2879	63399 $\pm$ 3406	47728 $\pm$ 3201	84582 $\pm$ 4308	76665 $\pm$ 3168	59979 $\pm$ 4744	64827 $\pm$ 3261	---	---	---	26500 $\pm$ 1991
<i>Nitzschia</i>	22333 $\pm$ 433	24464 $\pm$ 536	24481 $\pm$ 858	29924 $\pm$ 871	21659 $\pm$ 454	27923 $\pm$ 800	28496 $\pm$ 1514	19343 $\pm$ 469	54285 $\pm$ 777	52562 $\pm$ 2411	46052 $\pm$ 1087	34732 $\pm$ 1678
<i>Odontella</i>	88543 $\pm$ 3470	119426 $\pm$ 7719	160814 $\pm$ 11352	150331 $\pm$ 25214	64219 $\pm$ 1274	52293 $\pm$ 642	204436 $\pm$ 39396	464929 $\pm$ 46349	55628 $\pm$ 1713	43943 $\pm$ 1056	33572 $\pm$ 374	30158 $\pm$ 617
<i>Paralia</i>	67243 $\pm$ 2129	52560 $\pm$ 1926	74512 $\pm$ 4552	129900 $\pm$ 27700	48625 $\pm$ 985	64986 $\pm$ 3155	67400 $\pm$ 7642	64812 $\pm$ 6653	---	---	---	---
<i>Planktoniella</i>	38630 $\pm$ 13506	35406 $\pm$ 11755	28675 $\pm$ 3565	26200	---	28867 $\pm$ 920	37300 $\pm$ 1458	30158 $\pm$ 2218	---	25200 $\pm$ 3100	---	53422 $\pm$ 13037
<i>Pleurosigma</i>	93007 $\pm$ 2922	108014 $\pm$ 2638	112833 $\pm$ 4565	107542 $\pm$ 5925	153722 $\pm$ 3792	118108 $\pm$ 6323	109013 $\pm$ 18728	80290 $\pm$ 4562	97563 $\pm$ 1595	133000 $\pm$ 3805	159040 $\pm$ 2511	143712 $\pm$ 7099
<i>Pseudo-nitzschia</i>	16367 $\pm$ 202	11742 $\pm$ 187	14991 $\pm$ 231	18690 $\pm$ 550	18140 $\pm$ 413	10516 $\pm$ 299	6554 $\pm$ 389	7393 $\pm$ 366	17336 $\pm$ 184	14433 $\pm$ 476	17338 $\pm$ 516	10048 $\pm$ 460
<i>Rhizosolenia</i>	113437 $\pm$ 5911	117098 $\pm$ 5464	107960 $\pm$ 9294	119531 $\pm$ 7677	89897 $\pm$ 4164	103505 $\pm$ 4142	163144 $\pm$ 21494	106900 $\pm$ 6624	59339 $\pm$ 2177	67452 $\pm$ 2296	67385 $\pm$ 2337	45921 $\pm$ 1790
<i>Skeletonema</i>	18904 $\pm$ 134	14902 $\pm$ 313	15254 $\pm$ 336	16945 $\pm$ 504	17364 $\pm$ 54	15796 $\pm$ 61	25103 $\pm$ 856	23035 $\pm$ 412	9990 $\pm$ 142	12544 $\pm$ 194	12290 $\pm$ 105	12498 $\pm$ 206
<i>Streptothea</i>	120671 $\pm$ 4283	112953 $\pm$ 9557	147924 $\pm$ 19419	407223 $\pm$ 116436	126820 $\pm$ 11718	119016 $\pm$ 6252	209126 $\pm$ 37454	282486 $\pm$ 25240	123000 $\pm$ 16684	146000 $\pm$ 14250	---	---
<i>Surirella</i>	79936 $\pm$ 2774	61500 $\pm$ 4400	58300 $\pm$ 4258	32512 $\pm$ 1788	36025 $\pm$ 1239	34467 $\pm$ 705	36750 $\pm$ 3270	40280 $\pm$ 1133	---	39600 $\pm$ 2185	34167 $\pm$ 1520	---
<i>Thalassionema</i>	25870 $\pm$ 717	40449 $\pm$ 2692	33839 $\pm$ 3639	18033 $\pm$ 907	20274 $\pm$ 511	22935 $\pm$ 843	36816 $\pm$ 2694	51468 $\pm$ 1468	16923 $\pm$ 162	19762 $\pm$ 217	16294 $\pm$ 197	15900 $\pm$ 161
<i>Thalassiosira</i>	85849 $\pm$ 3761	124095 $\pm$ 5969	100314 $\pm$ 18576	203173 $\pm$ 17671	93099 $\pm$ 3220	114101 $\pm$ 10037	69752 $\pm$ 5842	88606 $\pm$ 4828	69067 $\pm$ 613	78110 $\pm$ 777	76509 $\pm$ 1065	96420 $\pm$ 3120
<i>Cyanobacteria</i>	---	554833 $\pm$ 334196	51100 $\pm$ 4993	120184 $\pm$ 12653	69205 $\pm$ 7097	436429 $\pm$ 44838	154608 $\pm$ 7203	195086 $\pm$ 11198	---	---	211000 $\pm$ 25485	83800 $\pm$ 16733
<i>Ceratum</i>	36931 $\pm$ 437	111868 $\pm$ 6221	174141 $\pm$ 16851	132360 $\pm$ 12205	49202 $\pm$ 338	195467 $\pm$ 7331	171583 $\pm$ 10122	181069 $\pm$ 7534	72893 $\pm$ 1961	135313 $\pm$ 7144	102079 $\pm$ 6163	169571 $\pm$ 11011
<i>Dimorphis</i>	24259 $\pm$ 701	52585 $\pm$ 3165	105109 $\pm$ 43723	56900 $\pm$ 3584	39383 $\pm$ 838	185318 $\pm$ 25963	191990 $\pm$ 35450	129922 $\pm$ 20892	33506 $\pm$ 169	41538 $\pm$ 983	67745 $\pm$ 5768	84408 $\pm$ 8535

<i>Oxytoxum</i>	---	---	7735± 75	8580± 1020	---	---	12433± 2339	7448± 467	---	---	---	---
<i>Prorocentrum</i>	18288± 467	17167± 370	18510± 738	16938± 255	21291± 241	21338± 795	24014± 1333	17993± 504	14600± 1054	21050± 1136	19860± 1453	20920± 1361
<i>Dictyocha</i>	19250± 1067	21286± 534	18278± 424	---	18927± 316	18171± 505	17813± 403	20008± 1645	19750± 584	15250± 424	18180± 457	15050± 1350
<b>Heterotrophs</b>	<b>NEM-1</b>	<b>NEM-3</b>	<b>NEM-5</b>	<b>NEM-7</b>	<b>PSWM-1</b>	<b>PSWM-3</b>	<b>PSWM-5</b>	<b>PSWM-7</b>	<b>SWM-1</b>	<b>SWM-3</b>	<b>SWM-5</b>	<b>SWM-7</b>
<i>Ornithocercus</i>	---	74127± 6753	84586± 3541	---	97278± 4191	84810± 2849	73400± 4300	79854± 1841	---	96775± 6963	74588± 4600	60713± 5114
<i>Gymnodinium</i>	37109± 275	47888± 3386	39822± 963	---	49497± 506	39326± 671	36946± 1041	41897± 625	---	67536± 2029	83613± 6651	73520± 1755
<i>Gyrodinium</i>	163000± 12954	123825± 15944	83000± 8018	110200± 3326	129444± 3172	74200± 7430	94842± 15007	116367± 16839	34600± 4581	---	27256± 1136	182500± 6500
<i>Noctiluca</i>	1850,000± 154739	605,000± 124855	1308,250± 224,417	---	1700,000± 32118	1446,333± 305898	643,000± 58488	297,000± 32965	---	---	---	---
<i>Podolampus</i>	---	20700± 1587	27450± 2387	---	21100± 350	29800± 245	---	23650± 34	---	---	34375± 846	26950± 2150
<i>Polytrikos</i>	96000± 3481	77600± 3260	---	---	91000± 3125	---	---	52900± 2715	---	75867± 3562	55700± 1569	72700± 2546
<i>Polysphaeridium</i>	---	704000± 78444	280300± 245700	401983± 232176	---	760455± 15311	639833± 70108	820200± 30549	---	---	208000± 23000	184000± 1574
<i>Protoperidinium</i>	62383± 1321	78828± 1986	66176± 1978	92208± 3797	64967± 693	78100± 2320	117801± 8911	95501± 3930	56994± 913	71908± 1323	86171± 4452	90386± 4928
<i>Stelladinium</i>	---	4410± 758	31700± 2485	---	---	---	---	19333± 928	---	5273± 385	30200± 4857	---
<i>Favella</i>	1280,000± 148247	---	933,000± 128462	---	851,667± 95733	---	---	---	326,000± 22418	1360,000± 132545	---	---
<i>Mesodinium</i>	---	---	---	72475± 9559	---	46600± 2544	---	---	---	74000± 3485	33067± 1785	25350± 972
<i>Strombidium</i>	22578± 421	---	25000± 433	19600± 364	15200± 1547	---	---	---	59325± 711	---	---	---
<i>Tintinnopsis</i>	100,333± 2062	118,850± 3270	131,929± 6369	100,515± 3157	110,189± 1674	60374± 2162	81576± 3094	104,715± 2338	62499± 1491	113,794± 7839	98748± 6971	146,264± 12239
<i>Foraminifera</i>	208,667± 5687	83213± 6112	82413± 12062	138,566± 13211	64367± 2738	93748± 5572	82726± 7850	69836± 2936	220,000± 16813	---	261,000± 19457	268,600± 21678
<i>Nauplius</i>	269,247± 7070	319,110± 15478	330,345± 13216	340,746± 12523	452,728± 14386	439,233± 21942	392,749± 20396	292,049± 10627	213,892± 4492	257,558± 6722	283,363± 10688	298,055± 6528
<i>Acanthometron</i>	83013± 7427	110,411± 13385	265,518± 108545	138,583± 15675	50567± 4919	182,241± 31979	276,658± 28563	498,156± 86526	---	143,000± 130485	861,567± 195213	342,165± 60713
<i>Radiolaria</i>	31830± 2572	85464± 32099	205,684± 106048	160,067± 67891	---	---	31117± 3719	---	---	---	24100± 2955	---